TAL TECH

A MOLECULARLY IMPRINTED POLYMER COMBINING m-PHENYLENEDIAMINE AND 3-AMINOPHENYLBORONIC ACID: TOWARDS THE DEVELOPMENT OF MACROLIDE-SELECTIVE MATERIALS FOR SENSOR APPLICATION

m-FENÜLEENDIAMIINI JA 3-AMINOFENÜÜLBOROONHAPE KOOSPOLÜMERISATSIOONIL PÕHINEV MOLEKULAARSELT JÄLJENDATUD POLÜMEER MAKROLIIDIDE SUHTES SELEKTIIVSETE SENSORMATERJALIDE VALMISTAMISEKS

MASTER THESIS

Student:	Vu Bao Chau Nguyen
Student code:	194295KAYM
Supervisor:	Vitali Sõritski Ph.D
Co-supervisor:	Akinrinade George Ayankojo Ph.D

Tallinn 2021

Non-exclusive licence for reproduction and publication of a graduation thesis[1]

I, Vu Bao Chau Nguyen

1.grant Tallinn University of Technology free licence (non-exclusive licence) for my thesis:

A MOLECULARLY IMPRINTED POLYMER COMBINING m-PHENYLENEDIAMINE AND 3-AMINOPHENYLBORONIC ACID: TOWARDS THE DEVELOPMENT OF MACROLIDE-SELECTIVE MATERIALS FOR SENSOR APPLICATION,

supervised by Vitali Sõritski Ph.D, and Akinrinade George Ayankojo Ph.D,

1.1 to be reproduced for the purposes of preservation and electronic publication of the graduation thesis, incl. to be entered in the digital collection of the library of Tallinn University of Technology until expiry of the term of copyright;

1.2 to be published via the web of Tallinn University of Technology, incl. to be entered in the digital collection of the library of Tallinn University of Technology until expiry of the term of copyright.

2. I am aware that the author also retains the rights specified in clause 1 of the non-exclusive licence.

3. I confirm that granting the non-exclusive licence does not infringe other persons' intellectual property rights, the rights arising from the Personal Data Protection Act or rights arising from other legislation.

_____

_____ (date)

Department of Materials and Environmental Technology
THESIS TASK

Student: Vu Bao Chau Nguyen, 194295KAYM

Study programme, KAYM09/18 - Materials and Processes for Sustainable Energetics

main speciality: Materials for Sustainable Energetics

Supervisor(s): Head of Laboratory, Vitali Sõritski Ph.D, vitali.syritski@taltech.ee;

Researcher, Akinrinade George Ayankojo Ph.D, akinrinade.ayankojo@ttu.ee.

Thesis topic:

(In English) A MOLECULARLY IMPRINTED POLYMER COMBINING m-PHENYLENEDIAMINE AND 3-AMINOPHENYLBORONIC ACID: TOWARDS THE DEVELOPMENT OF MACROLIDE-SELECTIVE MATERIALS FOR SENSOR APPLICATION

(In Estonian) m-FENÜLEENDIAMIINI JA 3-AMINOFENÜÜLBOROONHAPE KOOSPOLÜMERISATSIOONIL PÕHINEV MOLEKULAARSELT JÄLJENDATUD POLÜMEER MAKROLIIDIDE SUHTES SELEKTIIVSETE SENSORMATERJALIDE VALMISTAMISEKS

Thesis main objectives:

1. The selection of two functional monomers
2. The optimization of synthesis parameters
3. Evaluation of sensor rebinding
4. The study of group-selectivity

Thesis tasks and time schedule:

No	Task description	Deadline
1.	The selection of two functional monomers	Sep 2020
2.	The optimization of synthesis parameters	Nov 2020
3.	The optimization of synthesis parameters	Jan 2021
4.	The study of group-selectivity	Feb 2021

Language: English. **Deadline for submission of thesis:** "26" May 2021

Student: Vu Bao Chau Nguyen .....…........ "......."……….................. 2021

/signature/

Supervisor: Vitali Sõritski Ph.D ………………….. "......."..................... 2021

/signature/

Head of study programme: Sergei Bereznev Ph.D .... "........" 2021

/signature/

CONTENTS

PREFACE

This has been written not only to fulfil the graduation requirements of the TalTech University but also to share my personal interest in chemical sensors. I was engaged in researching and writing this thesis from September 2020 to May 2021.

The research was done at Biofunctional Materials laboratory, Department of Materials and Environmental Technology, TalTech. My thesis was written under the assistance and supervision of my supervisor, Dr. Vitali Sõritski, and my co-supervisor, Dr. George Ayankojo. The study was challenging, but conducting extensive experiments allowed me to address all of the issues that we established from the beginning. Fortunately, either my TalTech supervisors and tutors also were willing to answer my questions.

I'd like to express my gratitude to my supervisors for their excellent guidance and encouragement during the whole process. My thanks also go to everyone I've worked with in our department, particularly Dr. Roman Boroznjak and Dr. Jekaterina Reut, who are always friendly and ready to help.

In addition, I would like to thank Dr. Marina Kudrjašova from the Department of Chemistry and Biotechnology of TalTech University for her assistance with ^{13}C nuclear magnetic resonance spectroscopy.

Finally, I truly appreciate TalTech University, my supervisor Dr. Vitali Sõritski, and Dr. Sergei Bereznev for scholarships that allow me to focus on my studies, and additional educational opportunities.

Vu Bao Chau Nguyen

Keywords: Molecularly imprinted polymer; macrolides; antibiotics detection; group-selective MIP; master thesis.

List of abbreviations and symbols

AMO	Amoxicillin
APBA	3-aminophenylboronic acid
Azi	Azithromycin
CE	Counter electrode
Cipro	Ciprofloxacin
Cla	Clarithromycin
CV	Cyclic voltammetry
DPV	Differential pulse voltammetry
EIS	Electrochemical impedance spectroscopy
Ery	Erythromycin
gMIP	group-selective molecularly imprinted polymer
IF	Imprinting factor
MIP	Molecularly imprinted polymer
MIT	Molecular imprinting technique
mPD	m-phenylenediamine
NIP	Non-imprinted polymer
PBS	Phosphate buffered saline
RE	Reference electrode
SMZ	Sulfamethizole
SPE	Screen-printed electrode
WE	Working electrode

INTRODUCTION

Antibiotics are chemical compounds that inhibit the growth of microorganisms or kill them and are frequently used in healthcare and agriculture. The continuous release of the antibiotics into the environment [1,2] led to the production of antibiotic resistance in bacteria [3]. Antibiotic resistance constitutes major public health problems such as extended hospital stays, rising medical costs, and increased mortality [4]. Environmental sample analysis is mostly processed under laboratory conditions using high-performance liquid chromatography (HPLC), enzyme-linked immunosorbent assay (ELISA), mass spectrometry (MS) [5]. However, these traditional techniques need expensive instrumentation, well trained personnel and are not portable. Consequently, alternative analytical devices, such as sensors that detect antibiotics in water, are vitally important. The scientific community is exploring methods for improved analysis in order to detect the traces of antibiotics from natural waters [5,6]. Although certain progress has been recorded, difficulties in special conditions requirements, as well as the unstable natural receptors used in biosensors, impede their continued usage.

One approach to overcome this challenge involves the use of molecularly imprinted technology (MIT) that generates highly stable and selective artificial molecular recognition material called molecularly imprinted polymer (MIP). MIT is used to generate synthetic receptors through the creation of a polymer network around a chosen target molecule acting as a template. The subsequent removal of the templates from the formed polymer leaves behind binding sites that are complementary to the target molecule in size, shape and arrangement of functional groups. The established binding sites can detect the target and distinguish between molecules of similar structure [7]. MIP as a synthetic receptor has advantages including, simpler preparation, and better stability compared to biological receptors. MIP integration with various sensing platforms in order to produce low-cost accurate sensors for environmental monitoring have been extensively studied [8]. A number of studies have focused on the production of electrochemical MIP-based sensors since they provide desirable portability, real-time monitoring, and inexpensiveness [9,10]. Among pharmaceutical pollutants, antibiotics are the most commonly researched target analyte for electrochemical detection using MIP-based sensors [11]. Recently, Syritski's group has successfully achieved the portable and selective MIP-based sensor for electrochemical detection of erythromycin (Ery) inside aqueous media using m-phenylenediamine (mPD) as a single functional monomer [12]. Although clarithromycin (Cla) and azithromycin (Azi) have very similar structure to Ery, the generated Ery-MIP sensor did not show good response towards them. However, since the real environmental water sample contains all types of antibiotics presented usually at very low concentration, the possibility of group-selective

detection can be of great advantage. To address the need, group-selective MIPs (gMIP) capable of recognition of a group of closely related compounds rather than one constituent have been reported [13,14]. It was also found that applying a single template to synthesize gMIP helped to maximize time-efficiency and reduce the number of required templates in the preparation stage as compared to the multi-template synthesis approach [14].

This thesis aims to develop gMIP for the macrolide class of antibiotics (Ery, Cla, and Azi), which involves the use of two functional monomers during the synthesis process. The combination of two or more functional monomers for MIP synthesis can provide multiple recognition sites to different regions of the template improving the selectivity as compared to MIPs synthesized from a single functional monomer [15,16]. To reach the aim of the thesis, four objectives need to be fulfilled: the selection of functional monomers; the optimization of the synthesis parameters in order to produce a homogeneous polymer film on the sensor surface; evaluation of sensor rebinding; and study of group-selectivity of the prepared gMIP-based sensor. gMIP was prepared by electrochemical polymerization on the surface of a screen-printed electrode (SPE). Cyclic voltammetry (CV), differential pulse voltammetry (DPV), and electrochemical impedance spectroscopy (EIS) were used to monitor the polymerization as well as to evaluate the capability of the resulting gMIP to selectively recognize the chosen macrolides. The success of the research would add a significant contribution to the needed commercial sensors based on gMIP for the recognition of multiple target molecules belonging to the same group of compounds [13].

1. THEORY AND LITERATURE REVIEW

1.1 Environmental pollutants

1.1.1 Pollutants and water pollution

Environmental pollution is one of the most serious problems that we are facing today. Environmental pollution sources can be divided into natural and man-made [17]. Indeed, the huge amount of environmental pollution comes from our activities: not only social and economic structures but also the development of science and technology [18]. Pollutants are substances causing long-term and short-term effects on humans and the use of resources [19]. Those pollutants can be divided into organic, inorganic, thermal, noise, radioactive, and mixed pollution sources.

It is well known that the planet is saturated with 78% water, and our body contains more or less 70% water [20]. In living species, water plays important functions, including solvent, temperature barrier, metabolite, living environments, and lubricants [21]. Water contamination is a major topic facing the current generation as a global concern, and their effects can differ based on their type and source [17]. Water pollutants could be categorized into conventional and emerging. Conventional contaminants include fluoride (F^-), nitrate (NO_3^-, NO_2^-, NH_3^+), and heavy metals (Sb, Cu, Pb, Hg, Ni, Zn, etc) while emerging water pollutants include pharmaceuticals, endocrine disrupting compounds, artificial sweeteners, surfactants, etc [22]. All types of water pollutants negatively impact marine flora and fauna, disrupt the ecosystem, and affect human health issues.

1.1.2 Pharmaceutical pollutants

Pharmaceutical products, which are used for both humans and animals, are particularly important in their everyday lives. In addition, their presence in the water system is one of the most troublesome and persistent issues. The main sources of pharmaceutical contamination are processed waste from pharmaceutical plants, hospital waste, plant, and livestock treatment [23]. Due to population increase and massive intake of drugs the accumulation of pharmaceutical products in the aquatic ecosystem is growing. They can also accumulate in their original state or by-products in the additional sludge produced by the processes of treatment. It is worth noting that certain by-products can be more harmful than their compounds. The prolonged release of these substances and their long ambient exposures may have long-term (chronic) consequences [24]. Nowadays, pharmaceutical components have been shown to be abundant in surface

water, groundwater, and drinking water [25]. Among them, antibiotics as a large group of pharmaceuticals or drugs, are widely used in the treatment of infections.

1.2 Antibiotics

1.2.1 Antibiotic use and antibiotic resistance

Antibiotics are molecules with antimicrobial action, known to be a very effective type of pharmaceuticals used by humans in medicine, in animal treatment, poultry processing, and food security. They can either kill or prevent the growth of bacteria [26]. From the 1920s, the use of antibiotics in medicine has increased lifetime, made safer treatments and more patients can be easily recovered through bacterial diseases [27].

Since the 1900s, scientists have discovered that microorganisms were capable of resisting any of the drugs used. Most pathogens appear to be able to develop resistance to certain antimicrobial agents. These bacteria can infect humans and animals and are more difficult to manage than non-resistant [4]. The projected estimates indicate that the total intake of antibiotics used for agriculture would increase from 63000 to 105000 tons a year between 2010 and 2030 (approximately 67% growth), suggesting a significant jump in antibiotic resistance [28]. Furthermore, the speed of resistance is noticeable: as an example over 70% of S. Isolated Aureus resists erythromycin after 6 months of treatment [29]. There is a serious need for all countries to improve the way medicines are administered and used. The spread of antibiotic-resistant genes has become a global phenomenon and a multi-faceted danger. As a result of this situation, scientists have started to record and estimate the number of deaths as a result of bacterial antibiotic resistance. In 2009, the European Centre for Disease Prevention and Control (ECDC) reported that 25000 European deaths were caused by multidrug resistance. The US Center for Disease Control and Prevention (CDC) released a study in 2013 indicating that AR causes an additional 23000 deaths per year in the United States [30]. Eventually, researchers in 2016 predicted that antimicrobial resistance could cause 10 million deaths every year worldwide by 2050 [31]. All these data show that the detection of antibiotics in water environments is urgently necessary.

1.2.2 Antibiotic as pollutants in aqueous environments

In the majority of the environmental tests, antibiotics can be found deliberately released to the environment and result in significant detrimental effects on the habitat and humans. The existence of antibiotic residues in the water bodies threatens, directly and indirectly, community health. In aqueous environments, most antibiotics have limited solubility and antibiotic families, such as macrolides, are theoretically more likely to be

adsorbed by hydrophobic surfaces. This illustrates that it is very important to monitor and detect pharmaceutical pollutants, especially antibiotic agents. The international community is therefore mainly focusing on monitoring and removing antibiotics from wastewater [17,18].

The concentration and types of antibiotics in the water are different based on countries and courses. For example in Africa, the range of sulfamethoxazole in the surface water is 0,00027 – 39 µg/L [32]. In China, the mean and median concentrations found in purified tap water are 182 and 92 ng/L with 58 different antibiotics. In Chinese brand water bottles, they are 180 and 105 ng/L with 45 antibiotics. And in international bottled water brands, they are 666 and 146 ng/L with 36 antibiotics [33]. There are 17 antibiotics detected in treated industrial water effluent from 7 European countries (Spain, Portugal, Germany, Norway, Finland, Cyprus, and Ireland). Fluoroquinolones were reported to have the highest concentrations of antibiotics: ciprofloxacin in Portugal up to 1435,5 ng/L and ofloxacin 613 ng/L in Cyprus. In Portugal, the maximum concentrations of azithromycin and clarithromycin observed are 1577,3 ng/L and 346,8 ng/L [34]. Moreover, the "antibiotic pollution" happened not only in wastewater but also in drinking water [35]. Antibiotics most commonly found in aquatic ecosystems belong to the families of fluoroquinolones, beta-lactams, tetracyclines, sulfonamides, and macrolides [32]. Macrolide members including erythromycin (Ery), azithromycin (Azi), and clarithromycin (Cla) are on the EU surface water Watch List of emerging water toxins because of their widespread use and frequent detection in the environment. This list, which is updated every two years, contains all potential water pollutants that should be closely monitored by the EU Member States in order to assess the danger they pose to the aquatic environment [36].

1.2.3 Macrolide antibiotics

To people with penicillin allergies, macrolides including Ery and Azi were considered to be a supplement for β-lactam antibiotics. Besides the purpose of alternative for penicillin and working mostly on gram-positive bacteria, macrolides also have proven their usefulness in the prevention of some gram-negative infections or atypical pathogens [37]. Macrolide antibiotics are a validated class of antimicrobial agents that have played a major role in gram-positive bacteria chemotherapy [38,39]. They are distinguished by the appearance of a lactone macrocyclic ring carrying one or more residues of deoxy-sugar or amino sugar [40]. Many macrolides have been found, but only a few have been medically applied nowadays. Macrolide class features provide a relatively wide variety of antimicrobial operations, an orally efficient, and a reasonably high degree of safety [39]. For macrolides, the chemical composition includes a lactone ring of 12–18
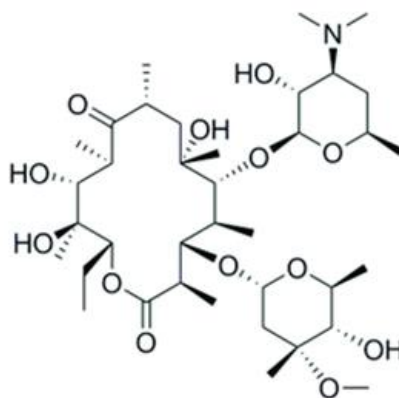
Figure 1.1. Molecular structure of erythromycin (C37H67NO13) [43].

members with direct or indirect links to 1–3 separate hexose moieties. One hexose moiety is connected to the position C5 of the ring [37]. Since the very first clinical use of Ery, more and more macrolides have been used in medicine such as Cla, Azi, josamycin, kitasamycin, roxithromycin, spiramycin, tilmicosin, tulathromycin, etc [41]. Within the scope of this thesis, only Ery, Cla, and Azi are used as target molecules.

Ery, discovered in 1952, is a 14-member ring macrolide (MW 733,9 g/mol) (Fig 1.1) [39]. It is effective toward gram-positive, gram-negative bacteria and various microorganisms [42].

Ery is quickly absorbed orally and transfers easily to the rest of the body fluids [42]. For 90% of organisms, the minimum inhibitory concentration is 0,13 mg/L and the minimum bactericidal concentration is 2,0 mg/L. This is higher than Ery concentration in environmental samples. It can be assumed that environmental levels of erythromycin for microorganisms are sublethal, therefore indicating a massive risk for antimicrobial resistance [28,44].

Cla (MW 748,0 g/mol) is used for the prevention of chest, skin, and ear infections. It also can be used for stomach ulcers caused by Helicobacter pylori. Cla is commonly used
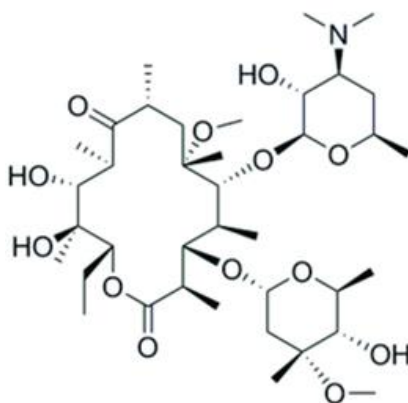

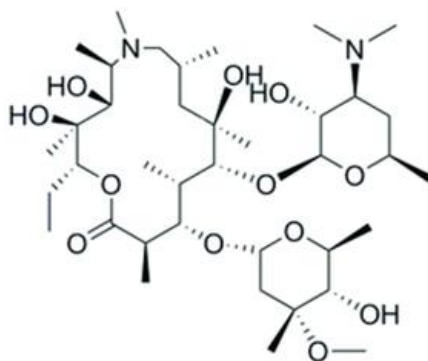*Figure 1.2. Molecular structure of clarithromycin (C38H69NO13) [43].*

Figure 1.3. Molecular structure of azithromycin (C38H72N2O12) [43].

for those with penicillin allergy. Cla, has enhanced bioavailability (50%) and adsorption among macrolides [45,46].

Azi (MW 749,0 g/mol) discovered in 1980, is commonly used to cure infections with pneumonia, nose and throat infections (mainly children), skin infections, Lyme disease, and some infections that are sexually transmitted. Including a methylated nitrogen atom at the ninth position of the macrolide lactone ring as shown in Fig. 1.3, it is active against gram-negative bacteria [47,48]. But with oral bioavailability of only 37% [45], it is easy to go into the wastewater system and pollute the environment.

1.3 Molecularly imprinted polymers

Over the last few years, there have been numerous studies and publications on molecular imprinting, which have been considered as a promising approach to develop artificial receptors. Molecularly printed polymers (MIPs) composed of strongly inter-linked polymers possess a biological structure-like recognizability in terms of the existence of unique sites that are complementary to a target molecule in structure and scale [49,50]. MIPs are also identified as plastic antibodies and similar to natural antibodies, with target molecule recognition features. MIP materials are more flexible mechanically and chemically, more robust, simple synthesis, easy to use [51]. The embodiments of MIPs have been performed in different shapes, for example, membranes, thin layers, nanoparticles, regular spherical particles, irregularly ground particles, composites, etc [45]. Therefore, MIPs have a broad variety of use, including sensors, chromatography, catalysis, sample pre-treatment, purification, and drug delivery [52–54].

1.3.1 Principle of molecular imprinting

MIP is formed by imprinting the template molecules in a polymer matrix followed by a washing procedure to have the template grooves. It reveals a preferred affinity with the

template molecule over others. This property is the primary driving force for all other applications [52].

The procedure of creating MIPs materials is described in Fig. 1.4. Affinity formation at the template active site can include several interactions, such as covalent interactions, electrostatic interactions, Van der Waals interactions, hydrophobic interactions, metal-center coordination. Following synthesizing, the removal of the template molecules is carried out leaving behind the "molecular memory" sites that are capable of selective recognition of the template molecule or its structural analogues [51,55]. Based on how templates interact with functional monomers, molecular imprinting approaches are categorized as covalent or non-covalent.

In a covalent approach, reversible covalent bonds between functional monomers and templates are established prior to the polymerization process. The complexes are stable with uniform distribution, and a broad range of conditions for polymerization are the main advantages of this approach [56,57]. The major disadvantage of covalent molecular imprinting is the limited number of functional monomers and templates that can be used to synthesize appropriate template-monomer complexes. Furthermore, due to the slow kinetics of template rebinding, this technique is unsuitable for applications requiring fast binding kinetics. To reduce the effect of negative factors, non-covalent or semi-covalent approaches can be used instead [58].

The non-covalent approach is now the most widely used method to prepare MIPs. This approach depends on many weak interactions between the functional monomers and
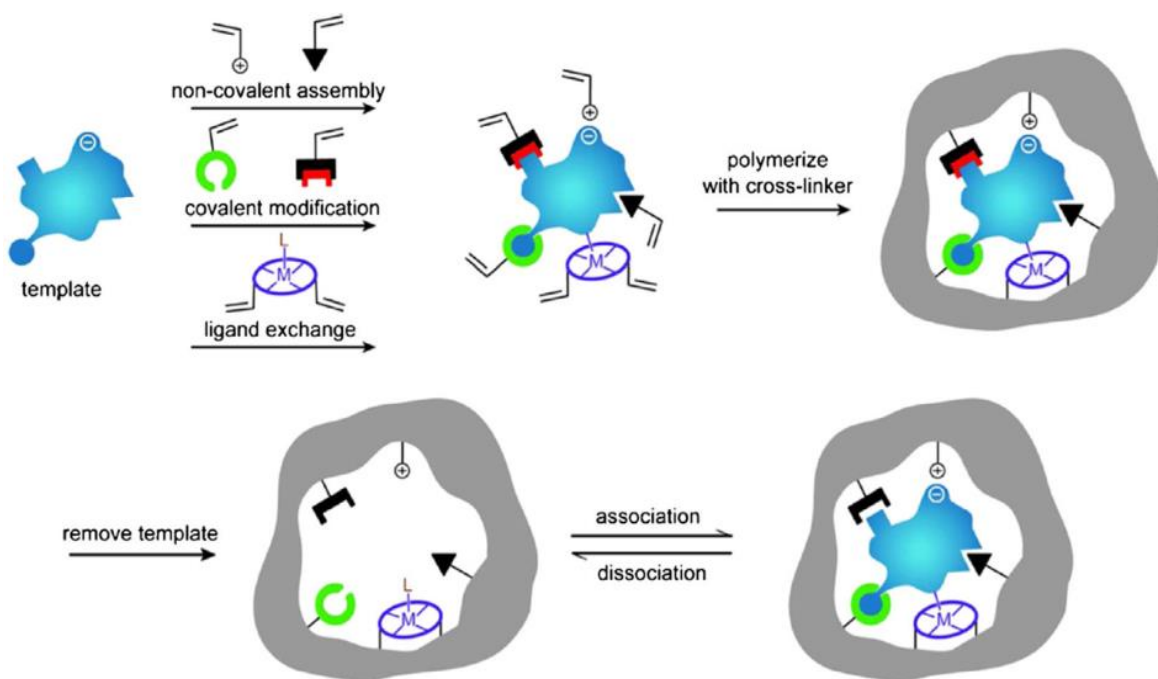

Figure 1.4. Schematic illustration of general molecular imprinting process [55].

the templates [59]. Commonly used non-covalent interactions are ionic, hydrophobic or hydrogen bond interactions. Without the formation and subsequent cleavage of chemical bonds, this approach made the removal process simpler as compared to covalent imprinting [55,57]. The main advantages of noncovalent imprinting include a large variety of functional monomers, high flexibility, low risk of template damage during polymerization, and rapid rebinding kinetics [58].

The third approach called "semi-covalent" is the combination of both covalent and non-covalent processes. During polymerization, the template is covalently bound to the functional monomer, but non-covalent interactions are exploited during the rebinding [59]. This means semi-covalent imprinting owns the advantages of both other approaches, the stoichiometric and stable complex and the quick binding with easy removal process [57].

1.3.2 Template molecules and functional monomers

The templates for molecular imprinting are selected depending on the MIP application purpose, namely the target molecule to be selectively recognized by the MIP. The templates can be biological molecules such as proteins, enzymes, amino acids, antibodies, bacteria, viruses, etc, or small organic/ inorganic molecules such as pesticides, antibiotics, metal ions, etc [60]. The three basic elements in the synthesis of MIPs are functional monomers, crosslinkers, and initiators. In order to construct highly selective cavities for the template molecule, the selection of a functional monomer is crucial. The optimal monomers for a noncovalent MIP synthesis are selected based on the consideration of the strength of interactions between functional groups of monomers and a template molecule. The cross-linker helps to manage the morphology of the MIP matrix [51,55,59].

1.3.3 Synthesis methods

Most often MIPs are prepared by free radical polymerization using a variety of methods, such as bulk, suspension, precipitation, and emulsion polymerizations. The latter three methods offer polymeric beads ready for various analytical applications, while bulk polymerization provides monoliths that need to be grinded in order to acquire smaller particles. Moreover, various synthesis approaches were introduced to prepare MIPs such as sol-gel method [61], surface imprinting [62], nanoscale imprinting [63] and solid-phase synthesis [64].

Electrochemically driven free-radical polymerization and sol-gel processing technology provide MIP production at room temperature with a possibility to integrate MIP films on a large number of different sensor transducers [65,66]. Electropolymerization is an

effective technique for producing morphologically controlled polymer films. It involves anodic oxidation of a monomer to obtain a radical cation [67]. These unstable radicals react easily with others, forming the polymer chain. With electropolymerization, polymer films with high adherence can be generated directly on the surface of conducting electrodes such as gold, platinum, glassy carbon, etc. The choice of monomer(s) and their ratio are critical to ensure its optimized performance [7,67]. The combination of two or more functional monomers that are complementary to different regions of the template has been used to improve multi-interaction between the template molecule and functional monomers. Multiple functional monomers imprinting strategy supplies multiple recognition sites to different regions of the template. When compared to MIPs synthesized from a single functional monomer, the MIPs prepared by this strategy have a significantly improved imprinting effect and a higher adsorption capability [15,68]. In this work, the copolymerization of two functional monomers, m-phenylenediamine (mPD) and 3-aminophenylboronic acid (APBA) was used to prepare MIP films possessing higher selective recognition cavities towards the analyte.

1.3.4 Group-selective MIPs

Recently, class-selective MIP or group-selective MIP (gMIP) were developed [13,16], which allows molecularly recognized groups of structurally similar molecules. In the synthesis process, the use of a single template as a substitute for a whole group takes full advantage of similar molecular structures among compounds. This method optimizes the preparation steps and reduces the needed template amount. This phenomenon is useful, particularly for polychlorinated aromatic compounds that occur as congeners or homologs, gMIPs will result in their enrichment and detection at the same time [69]. In natural waters, all the macrolides exist together, and more are posing a threat to humankind due to the emergence of antibiotic resistance. Researchers are working to look for better solutions with the possibility of deploying the newly developed technology, more reliable and cheaper to detect macrolides. Recently, the Ery detection method with real-time monitoring by preparing a MIP-based electrochemical sensor was developed by Syritski's group. This thesis is aimed to extend the application of the gMIP-sensor by developing a macrolide group-selective MIPs integrated with an electrochemical transducer.

1.4 MIP-based sensor for pollutant detection

A chemical sensor, which includes a recognition element and transducer, is a device that detects an analyte by transforming the chemical interaction into measurable signals [60]. To construct sensors, MIPs as recognition elements are integrated with a large

number of various transducers. There are many different types of MIP- sensors classified based on the physical properties of the sensor transducer such as electrochemical, optical, magnetic, thermal, piezoelectric sensors [8]. The reliable interfacing of a MIP layer with a transducer can be accomplished with the aid of different methods including, for example, surface-initiated controlled/living radical photopolymerization [70] and electropolymerization [7]. The latter method has the advantages of the easier on-step synthesis, the possibility of a fine control of the polymer thickness by changing the total charge flowing at the electrode and high reproducibility. The environmental pollutants detection sensors are applied for aqueous media, some of them are used in the gas phase [71].

1.4.1 Electrochemical sensors

MIP-based electrochemical sensors have many advantages, including ease of preparation, high selectivity, portability, and inexpensive cost [72]. In case of electrochemical MIP-based sensors, a typical three-electrode setup with a MIP-modified working electrode gives signals when contacted with target molecules [7,73]. The changes of electrical signals (mostly current or potential) relative to the target analyte concentration are recorded. When analyte molecules rebind to the MIP film, they block the pathway of ions, resulting in a reduction in redox marker permeation (Fig. 1.5) [72]. Many electrochemical techniques, such as CV, EIS, and DPV can be used to evaluate the permeation of redox-active markers [74].

The electrochemical MIP-based sensors for detection of heavy metals, pesticides, pharmaceuticals, and other pollutants from water samples have been reported [11]. Numerous studies about MIP-modified electrochemical transducer have been reported to detect emerging contaminants such as gold electrode (to detect 17β-estradiol) [75],
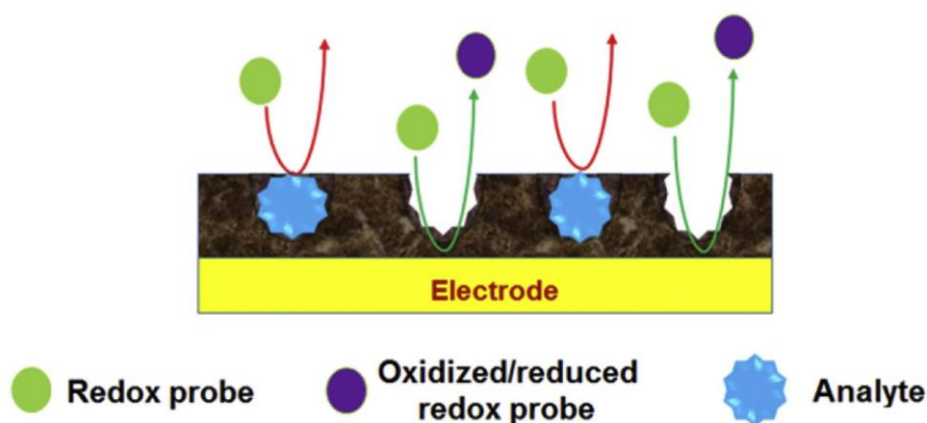

Figure 1.5. Illustration scheme of analyte molecules that prevent the redox probe from diffusing by filling the imprinted cavities [72].

boron-doped diamond electrode (cefalexin) [76], screen-printed electrode (ion Cu) [77], glassy carbon electrode (N-nitrosodimethylamine) [78], ect. In this work, Screen Printed Electrodes (SPE) was chosen as a low-cost electrochemical transducer to combine with a MIP layer.

1.4.2 Screen-printed electrodes

In past years, Screen Printed Electrodes (SPEs) have been widely used as electrochemical sensing platforms due to the affordable prices and easy-to-use. Another benefit associated with SPEs is the reduction of sample volume up to microliters that helps decrease the total size of the diagnostic instrument. SPEs are perfectly suited for the development of portable devices performing rapid and accurate in-situ analysis [79].

A standard SPE is made from a chemically inert substrate such as plastic or ceramic and three electrodes, working electrode (WE), reference electrode (RE) and counter electrode (CE), respectively, as shown in Fig. 1.6. The WE is the key electrode that offers an analyte recognition platform. The CE and RE are surrounded to complete the circuit. The most widely used pastes for printing SPEs are silver ink and carbon ink. WEs are mainly printed with graphite carbon inks, while other materials including gold, platinum inks, etc. also can be used to prepare SPEs depending on requirements and applications [80,81]. Carbon ink is a popular material because it can be modified, chemically inert, and fairly inexpensive. Gold is a better conductor, so the gold paste is also often used but at a higher price than carbon. Gold electrodes SPEs are employed for some specific purpose such as electrochemical biosensors when working with enzymes, protein, etc [79,80].
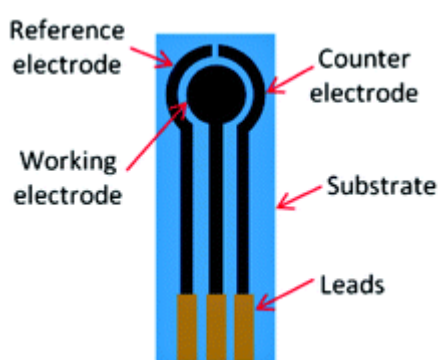

Figure 1.6. Representation of a SPE including three electrodes (WE, RE, and CE).

1.5 Experimental methods

1.5.1 Cyclic voltammetry

Cyclic Voltammetry (CV) is an effective electroanalytical technique commonly used to monitor electrochemical processes occurring on the surface of a conductive electrode at the molecular level [82]. It is a useful method for the rapid determination of the thermodynamics of redox processes. CV provides qualitative details about electrochemical processes under different conditions, such as the intermediate roles in oxidation-reduction reactions and the reversibility of a reaction. Furthermore, cyclic voltammetry can be used to study the electrical charge transfer blocking properties of insulating film-modified electrodes [83].

Cyclic voltammetry experiments are usually conducted in an electrochemical cell consisting of the electrolyte solution and three electrodes including WE, RE, and CE. A potentiostat is used to linearly sweep the potential between reference and working electrodes till reaching the preset limit then sweep in the opposite direction. During this process, the chemical can lose electrons (oxidation) or obtain electrons (reduction) based on the direction of the sweeping potential [82,83]. Fig. 1.7 shows the relationship between the applied potential, E and current I. The shape of 2 peaks came from equilibrium which is described by the Nernst equation (Eq. 1.1).

The Nernst equation defines the equilibrium formed between the oxidized (Ox) and reduced (Red) electrodes. The potential (E) of an electrochemical cell in relation to the
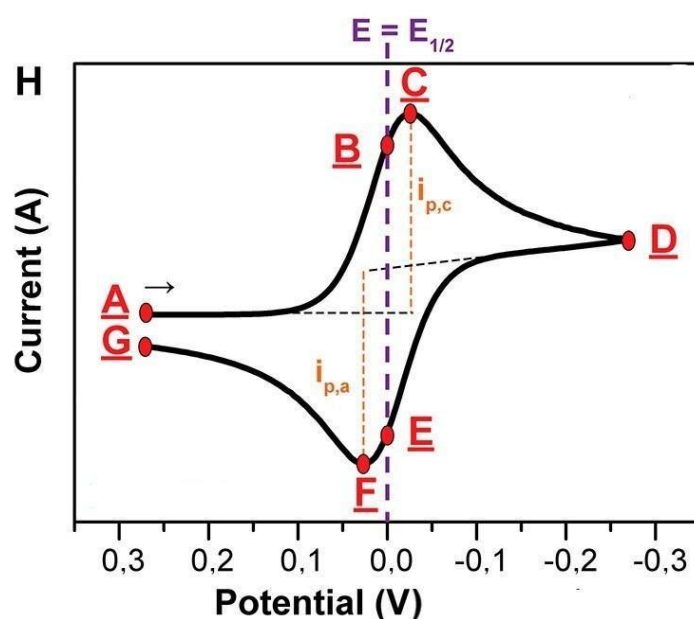

Figure 1.7. (A–G): Initial potential applied (A), Reduction peak (C), Higher potential limit (D), Oxidation peak (F), taken from [82].

normal electrode potential (E_0), and the relative behavior of the oxidized (Ox) and reduced (Red) analytes in the system at equilibrium:

$$E=E_0 + (RT/nF)\ln(Ox/Red) = E_0 + 2{,}3026(RT/nF)\log(Ox/Red) \qquad (1.1)$$

where E is the electrode potential, $E°$ is the standard potential of the electrode (for 1M solution at 298 K), F is Faraday's constant (96500 coulombs/mol), R is the universal gas constant (8,314 J/K·mol), n is the number of electrons accepted during the change, and T is the temperature (K).

1.5.2 Differential pulse voltammetry

Differential Pulse Voltammetry (DPV) is a sensitive pulse technique that helps minimize the background effects and allows analysis down to the nanoscale. By this method, potential pulses are applied to the electrode after the initial potential is maintained for a specified period of time. The current is sampled just before and after pulse application and their difference is recorded in order to establish a DPV graph. Fig. 1.8 shows a typical DPV voltammogram consisting of the plot of recorded current versus the applied potential. The current peak is directly proportional to the concentration of the analyte at a close proximity to the electrode [84–86].
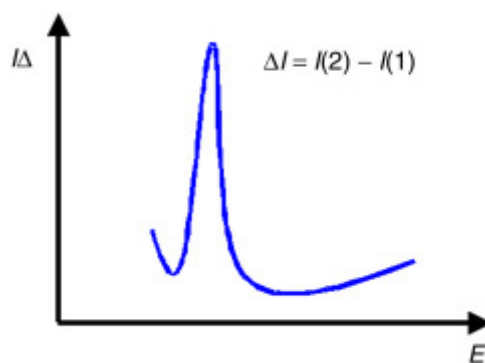
Figure 1.8. The typical response of current from applied pulse potential, taken from [86].

1.5.3 Electrochemical impedance spectroscopy

Electrochemical Impedance Spectroscopy (EIS) is a powerful technique that has been used for over a century for purposes such as surface analysis, adsorption properties in the molecular level, and monitoring the operation of fuel cells and batteries as well as biomedical applications [87,88]. EIS involves the study of materials with ion conduction involving the movement of electron or ion vacancies [88]. The main advantages are high precision and sensitivity, EIS is a non-invasive technique and simple instrument, easy operation, and especially does not require the bulk size of materials [87,89].

Electrochemical impedance is generally calculated by applying the AC potential and then by measuring the current through the system and finally determining the impedance $Z = E/I$ with a unit of Z in Ω. The impedance is defined in terms of magnitude (Z_0) and phase shift (φ) as (Eq. 1.2).

$$Z = E_t/I_t = E_0\sin(\omega t)/I_0\sin(\omega t+\varphi) = Z_0\sin(\omega t)/\sin(\omega t+\varphi) \qquad (1.2)$$

where E_t is potential at time t, I_t is current at time t.

Impedance is a complex number that is achieved by mathematical transformation. In the complex equation, the real part represents the resistors and the imaginary part represents the input of the capacitors and/or inductors.

$$Z(\varphi) = E/I = Z_0\exp(j\varphi) = Z_0(\cos\varphi+j\sin\varphi) \qquad (1.3)$$

with:

$$Z = Z'+jZ''=R - jX$$

$$X=1/\omega C$$

$$j=\sqrt{-1}$$

where R - the resistance (Ω), C - the capacitance (F), X - the reactance, and ω - the applied angular frequency (rad/s).

Nyquist plot is the plot where the real component Z' is displayed on the X-axis and the imaginary part Z'' is plotted on the Y-axis (Fig. 1.9.a). In this plot, two processes are distinguished, the first part is a semicircle corresponding to a charge-transfer-controlled process, where values on the Z' axis gives R_e and R_{ct} values; the second part is a line with a slope of 1 because Zw extrapolated to the X-axis allows the measurement of the Warburg coefficient (σ), which allows estimating the electroactive species diffusion coefficients.

The Randles circuit (Fig. 1.9.b) is the most basic, describing a cell where a single-step Faradaic phase occurs. R_e indicates the electrolyte resistance between the working and reference electrodes, C_{dl} expresses the double-layer capacitance, and Z_f is the Faradaic impedance induced by the charge-transfer mechanism at the electrode-electrolyte interface. Z_f is further known as charge-transfer resistance (R_{ct}) and Warburg Impedance (Z_w). Warburg Impedance reflects the effect of electroactive species mass
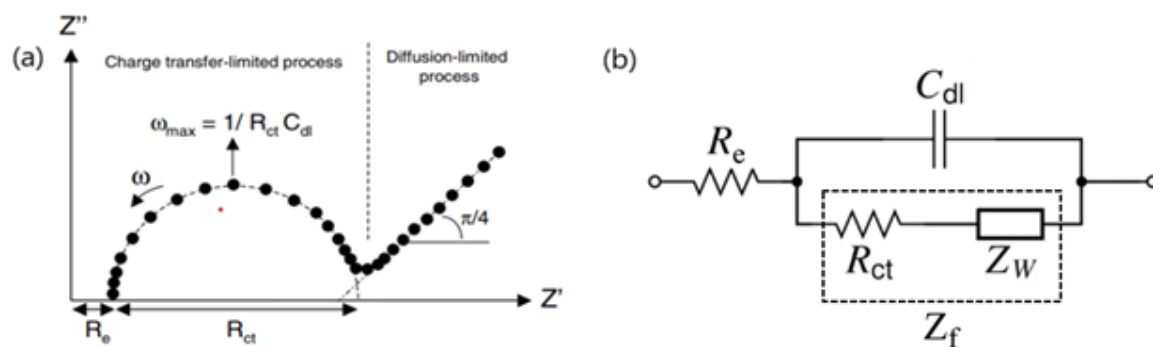
Figure 1.9. (a) Nyquist Plot, where each dot indicates the impedance at a specified frequency. (b) Randles equivalent circuit.

transfer. In this report, EIS is used as an estimation of the presence and thickness of the synthesized polymer layer on the working electrode [88,90,91].

1.5.4 Characterization of imprinting success

There exist several methods specially developed to prove the formation of molecular imprints during the MIP synthesis protocol. A common practice is to synthesize another polymer called non-imprinted polymer (NIP) along with a particular MIP. The NIP is used as a reference to estimate the relative adsorption capacity and whether the cavities formed in the MIP matrix are indeed selective to the analyte. After synthesis steps, MIP and NIP should be spent through the same procedures and be characterized. Prior experiments have shown that the chemical and physical differences between NIPs and MIPs can be remarkable. Thus, MIPs are usually more porous due to the presence of imprinted cavities. NIP can be seen as background providing information about non-specific binding [59,60]. The imprinting factor (IF) is used to evaluate the effectiveness of the imprinting process. IF is usually explained as the ratio between the analyte amount bound to MIP and the analyte amount bound to NIP. To calculate IF, a rebinding of the analyte on both NIP and MIP surfaces is studied and the adsorption isotherms are plotted. Adsorption isotherms reflect the dependency of a bound target's equilibrium concentration on the target concentration inside the solution and provide valuable information on the film's binding features [51,64,92]. In order to extract the binding parameters such as the maximal amount of adsorbed analyte and dissociation constant (K_D), the adsorption isotherms are fitted to mathematical models such as Langmuir, Freundlich and combined Langmuir-Freundlich (LF). The LFI model was proved to match the practical adsorption isotherms of MIPs better than either the Langmuir or Freundlich models [12,93]. The LF isotherm is a mathematical model that determines the relationship between analyte concentrations in bound and free states in heterogeneous environments (Eq. 1.4) [94,95].

$$Q = Q_{max}C^m(K_D + C^m) \qquad (1.4)$$

where *Q* and *Q_{max}* are the fraction of MIP bound analyte and its saturation value, respectively; *C* is the concentration of an analyte in a solution; *m* is the heterogeneity index, which ranges from 0 to 1; *K_D* is the dissociation constant at equilibrium. The LFI has been used successfully to simulate the adsorption activity of many heterogeneous structures such as gas adsorption from surfaces [96], affinity to polyclonal antibodies [97], metal ion adsorption [98] as well as MIP and NIP when the heterogeneity index m is lower than 1 [93,94]. One of the most appealing aspects of using the LF binding model to study MIPs is that the binding parameters such as mean binding affinity, and heterogeneity can be determined directly [93].

2. EXPERIMENTAL

2.1 Chemicals and materials

All the used chemicals listed in table 2.1, besides acetic acid given by Lach-ner, were purchased from Sigma. The chemicals were received and stored under standard conditions. The aqueous solutions were prepared with ultrapure water (resistivity 18,2 MΩcm, Millipore, USA). Buffered phosphate saline PBS, (0,01 M, pH 7,4) was used in preparing all analyte solutions. Gold-coated screen-printed electrodes (Au-SPEs), model AC1, were obtained from BVT technologies (Czech Republic). Au-SPE includes a 1 mm diameter circular Au working electrode, a silver reference electrode covered by AgCl, and a gold counter electrode.

Table 2.1 List of chemicals used for this thesis' experiments.

Short name	Components	Purpose
PBS	Phosphate buffered saline solution (0,01 M, pH 7,4)	Solutions for synthesis and analysis
Redox probe	$K_3[Fe(CN)_6]/K_4[Fe(CN)_6]$	Solutions for CV, EIS, and DPV measurements
AA10%	Acetic acid 10%	Template removal
mPD	2-Methyl-2,4-pentanediol $((CH_3)_2CCH_2CHCH_3)$	Functional monomer
APBA	3-Aminophenylboronic acid	Functional monomer
NaF	Sodium fluoride	Boronic acid-1,2-diol stabilizing agent
Ery	Erythromycin, macrolide antibiotic	Template, target analyte
Cla	Clarithromycin, macrolide antibiotic	Target analyte
Azi	Azithromycin, macrolide antibiotic	Target analyte
Cipro	Ciprofloxacin, fluoroquinolone antibiotic	Interfering compound for the selectivity study
Amo	Amoxicillin, β-lactam antibiotic	Interfering compound for the selectivity study
SMZ	Sulfamethizole, sulfonamide antibiotic	Interfering Compound for the selectivity study

2.2 Nuclear magnetic resonance spectroscopy

[13]C nuclear magnetic resonance spectroscopy was carried out with the Bruker SMART X2S benchtop diffractometer model at the Department of Chemistry and Biotechnology of Taltech University. Samples were prepared in acetonitrile (ACN) solution as solvent. A molar ratio of 1:1 (Ery: APBA) was for the study.

2.3 Protocols for gMIP film preparation

gMIP is prepared on a working electrode of the Au-SPE following 2 main stages including electrochemical polymerization of mPD and APBA in the presence of Ery, Ery template
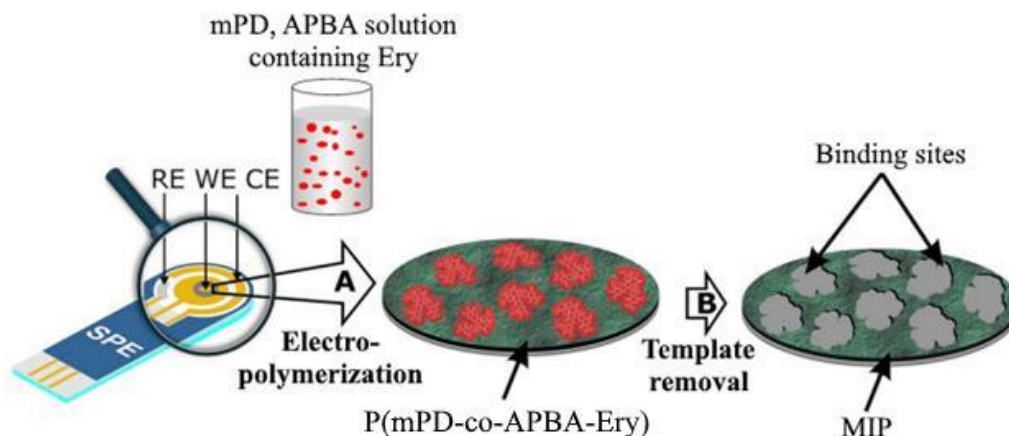
Figure 2.1. Schematics of the protocols for gMIP film formation on the Au working electrode of SPE, including A (Electropolymerization) and B (Template removal). At first, the SPE was processed by electropolymerization (A) in a solution containing mPD, ABPA, and Ery to form P(mPD-co-APBA-Ery). Secondly, the PSE with polymer layer on WE continued to go through template removal (B) in order to establish gMIP with binding sites. Finally, gMIP was ready for the rebinding stage [12].

removal (washing out) from the polymer matrix. Finally, the rebinding step was processed with Ery, Cla, Azi. All experiments were carried out at room temperature.

2.3.1 Electrodeposition of P(mPD-APBA)-Ery film on SPE

Before electrodeposition, the new SPE was cleaned electrochemically in 0,1 M sulfuric acid solution by cycling the potential between 0,1 and 1,15 V at a scan rate of 100 mV/s for 15 cycles. To synthesize the polymer film, a constant potential of 0,5 V vs Ag/AgCl was applied to the working electrode of the SPE that is immersed in a PBS (pH 7,4) solution containing 10 mM mPD, 5 mM APBA and 2 mM Ery. These concentrations were determined during the optimization stage of gMIP preparation. Similarly, the NIP was prepared analogously to gMIP but excluding the addition of Ery in the synthesis solution. The thickness of both polymer films was controlled by the amount of electrical charge transmitted through the WE. This helps to ensure the formation of reproducible films at all times while also achieving similarity in the thickness of both gMIP and NIP.

2.3.2 Template removal

To remove the entrapped Ery molecules within the polymer layer, the polymer-modified SPE was immersed in 1 mL 5% acetic acid solution for 30 min. The acidic environment helps to break the boronate ester bonds between APBA and Ery as well as to dissociate the non-covalent hydrogen bonds between mPD and Ery.

2.4 Characterization of gMIP preparation

The different stages of gMIP preparation were monitored with electrochemical techniques such as differential pulse voltammetry (DPV), electrochemical impedance spectroscopy (EIS), and cyclic voltammetry (CV). All electrochemical measurements were performed with the SPEs from BVT of Czech Republic and were connected with an electrochemical workstation called potentiostat (model Reference 600, Gamry Instruments, USA) and connector ordered from Palmsens of Netherland (model PS-CONN).

2.4.1 Cyclic voltammetry

CV measurements were conducted in a 1 M KCl solution containing 4mM redox probe $K_3[Fe(CN)_6]/K_4[Fe(CN)_6]$. The potentials were cycled between 0 and 0,5 V at a scan rate of 100 mV/s. Each sensor was subjected to at least three scanning cycles.

2.4.2 Electrochemical impedance spectroscopy

EIS experiments were performed in a 1M KCl solution consisting of 4 mM $K_3[Fe(CN)_6]/K_4[Fe(CN)_6]$ redox probe. An alternating potential with a 10mV amplitude and a frequency range of 0,1Hz to 100kHz were used. After at least three repeat times, the results were conducted. Using the equivalent circuit program included in Gamry Echem Analyst software, the impedance spectra were fitted to an equivalent electrical circuit.

2.4.3 Differential pulse voltammetry

DPV measurements have been performed in a 1M KCl solution containing 4mM redox probe $K_3[Fe(CN)_6]/K_4[Fe(CN)_6]$. DPV readings were done in the potential window between 0V and 0,4V with a pulse amplitude of 0,025V, a pulse width of 0,1s, a step potential of 0,005V, and a sample time of 0,5s.

The current peak values of DPV were normalized using (Eq. 1.5) to acquire the gMIP response signals (I_n) [51,64,92].

$$I_n = (I_0 - I)/I_0 \qquad (1.5)$$

where I_0 is the peak value measured by DPV before rebinding, and I is the peak value measured by DPV after rebinding. Both I_0 and I are recorded at the equilibrium state and have units in Ampe (A).

2.5 Rebinding study

To determine the performance of the prepared gMIPs, the sensors were tested for its rebinding capability at varying concentrations of the analytes. This was accomplished by recording the analyte-induced signals after incubating the sensor in analyte solution samples. A similar procedure was carried out with the NIP sensor to ensure the correct analysis of target induced response occurring on the gMIP sensor.

Individual solutions of each analyte (Ery, Cla, Azi) were prepared at different concentrations: 1,6 µM, 8 µM, 40 µM, 200 µM, and 1000 µM. Prior to the rebinding of each analyte, the sensor was incubated in PBS solution (blank) for 10 min and the DPV baseline was obtained in redox solution following its stabilization. Subsequently, the sensor was incubated for 10 min in the analyte solution starting with the lowest concentration before the DPV measurements. The adsorption isotherms representing the relationship between the increase of analyte concentration C and sensor response I_n were plotted and fitted by the LF model (Eq. 1.6).

$$I_n = I_{max}C^m(K_D+C^m) \tag{1.6}$$

where I_n and I_{max} are sensor response signals after adsorption of the analyte at the concentration C and its saturation value, respectively; m is the heterogeneity index; and K_D is equilibrium dissociation constant.

The IF value was calculated from equation (1.7).

$$IF = I_{max}(gMIP)/I_{max}(NIP) \tag{1.7}$$

3. RESULTS AND DISCUSSION

3.1 gMIP synthesis

3.1.1 Functional monomers selection

The performance of a MIP in selective binding of the target depends on the binding strength between functional monomers and a template molecule in the pre-polymerization complex that enables molecular memory in the polymer matrix. Therefore, in order to select suitable functional monomers for a target/template molecule, the stability of the monomer-template non-covalent complex or the possibility of the formation of a reversible covalent bond between a monomer and a template should be carefully assessed. The computational calculations conducted in the previous study [12] revealed that mPD (Fig. 3.1a) is an optimal functional monomer for Ery by forming the non-covalent complex via the hydrogen bonds between mPD (the amino groups) and Ery (hydroxyl-, carbonyl, and carboxyl groups). In addition, it was also shown that the electropolymerization of mPD (Fig. 3.1a) resulted in a very homogeneous and stable polymer film (poly(mPD)) as well as the subsequently prepared MIP having the high recognition capacity towards Ery. At the same time, mPD-based MIP demonstrated significantly lower response towards the other macrolides such as Cla and Azi [12]. Therefore, in order to prepare a MIP capable of selective binding of larger numbers of macrolide group antibiotics, e.g. gMIP, the selection of functional monomers should be optimized. The imprinting strategy involving the use of multiple functional monomers could represent a promising solution to achieve the aim.

Thus, in this study, 3-aminophenyl boronic acid (APBA) was chosen as the second functional monomer for gMIP synthesis to endow the gMIP with selective properties for
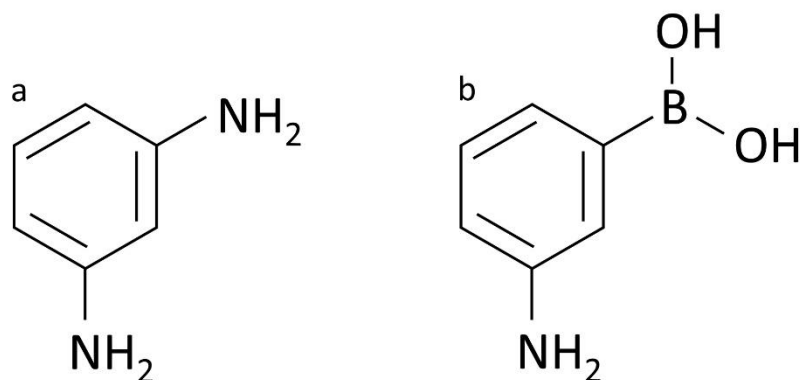

Figure 3.1. (a) Molecular structure of m-phenylenediamine (b) Molecular structure of 3-aminophenyl boronic acid.

macrolides (Ery, Cla, and Azi) recognition. APBA is an aniline derivative containing a boronic acid functional group (Fig. 3.1b).

Boronic acid can form reversible covalent bonds with 1,2 or 1,3 diols containing compounds [99,100]. At a neutral pH or higher (pH ≥ 7), boronic acid of APBA transforms into an anionic tetrahedral acidic molecule that can directly interact with 1,2-diols of neighbouring molecule (e.g Ery) to form a boronate ester covalent complex (Fig. 3.2). The complex reversibly dissociates when decreasing pH to the range of 5 - 2 [101].

The chemo-selective ability of APBA towards diol-group containing compounds has been widely used in sensors intended for detection of saccharides, glycated-proteins, nucleotides compounds, and bacteria [103,104]. Nevertheless, phenylboronic acid-based detection devices have many shortcomings, such as low stability and sensitivity, and difficulty separating background noise signals [105,106].

To study the interaction between APBA and 1,2-diol groups of Ery, the ^{13}C nuclear magnetic resonance (NMR) spectroscopy was carried out to observe and strengthen the reason for choosing APBA. NMR spectroscopy is a reliable tool for analyzing mixtures at the molecular level without the need for isolation or purification steps [107,108].
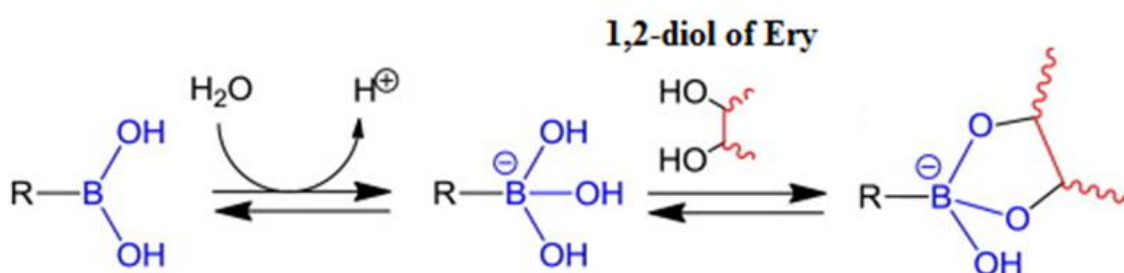

Figure 3.2. Interaction of boronic acid and 1,2-diols in the aqueous phase [102].

The characteristic spectra of either Ery or APBA is clearly seen in the solution of individual molecules (Fig. 3.3). However, the spectra of their mixture at pH 7,4 revealed the disappearance of Ery characteristic peaks in the range 25-100 ppt, while these peaks are still visible on the spectra of mixture at pH 4. This indicates the formation of a covalent bond between Ery and APBA at pH 7,4 and the cleavage of this bond at pH 4. Thus, the spectroscopic study confirmed that APBA is a suitable functional monomer for Ery imprinting by covalent approach.
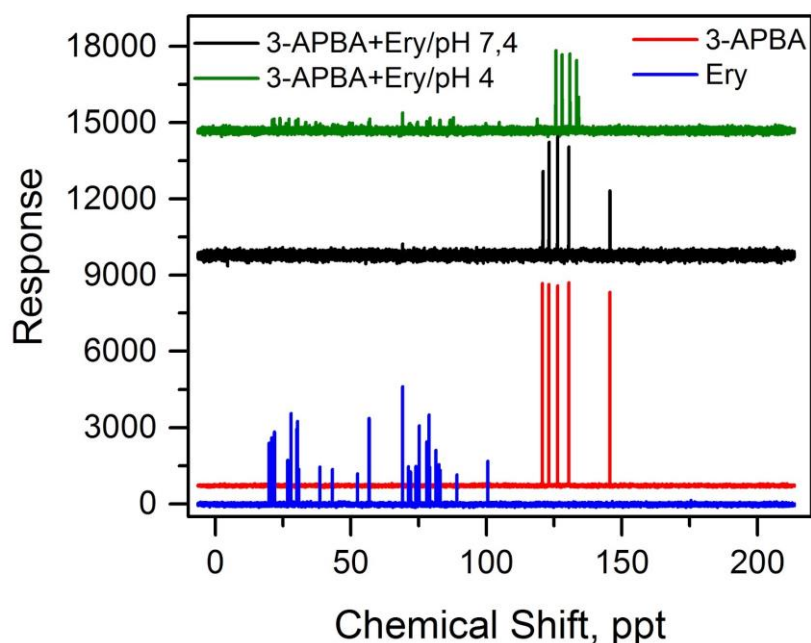
Figure 3.3. Liquid-state ^{13}C NMR spectroscopy of Ery, APBA and their mixture (molar ratio 1:1) at different pH.

Although the combination of APBA and mPD has been reported before to prepare aerogel for silver separating purposes [109], to the best of author's knowledge, this is the first time it is applied for preparing gMIP for group antibiotic recognition. The combination of two or more functional monomers for gMIP synthesis can provide multiple recognition sites to different regions of the template improving the selectivity as compared to gMIPs synthesized from a single functional monomer.

3.1.2 Selection of electropolymerization potential

The co-polymerization of the selected functional monomers, mPD and APBA, in the presence of Ery was initiated electrochemically by applying a constant potential to the gold working electrode of the SPE and resulting in the formation of polymer film P(mPD-co-APBA-Ery) on the electrode. It is important to guarantee that the template molecules were not oxidized at the electrodeposition potential of the chosen monomers in order to maintain their structure. As a result, the CV analysis was performed to assess oxidation potentials of the template (Ery) and monomers (mPD, APBA). The CV scans (Fig. 3.4) indicated that the mPD and APBA monomers started oxidizing at about 0,3 V and 0,4 V, respectively, while Ery - at about 0,6 V. Due to the similar oxidation potentials of the two monomers, it is possible to synthesize the copolymer from the two monomers since the electrochemically formed radical cations of both monomers could combine together to create a copolymer [89]. Thus, electrodeposition was performed at a fixed potential
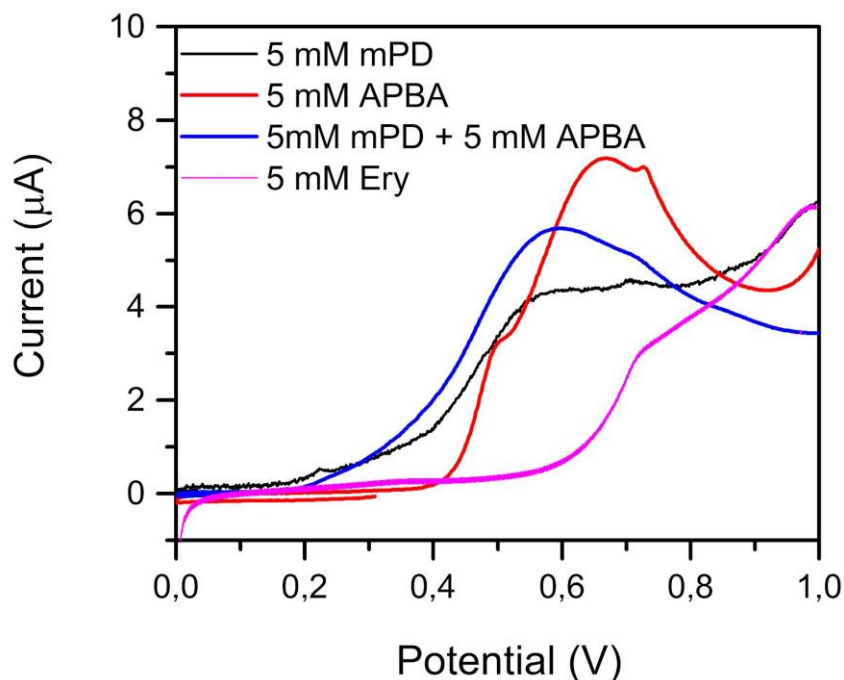
Figure 3.4. CV scans of 5mM mPD, 5mAPBA, 5mM mPD + 5mM APBA, 5mM Ery respectively.

of 0,5 V to ensure the formation of P(mPD-co-APBA-Ery) without affecting the structure of template molecules.

3.1.3 Characterization of gMIP formation process

EIS and CV measurements were performed at every stage of Ery-gMIP preparation (Fig. 3.5) to observe the changes in charge transfer at the electrode/solution interface induced by the modification of SPE surface. The anodic and cathodic current peaks of CV suffered significant depression following electrosynthesis of poly(mPD-co-APBA-Ery) indicating the formation of a non-conducting film that obstructs charge transfer (Fig. 3.5a). However, after acetic acid treatment, a substantial recovery of the peaks was observed, suggesting the removal of entrapped Ery molecules from the formed polymer. The similar behavior is observed with EIS spectra (Fig. 3.5b), where the semicircle, which represents the charge transfer resistance, greatly increased after electrosynthesis, followed by a subsequent decrease after treatment in acetic acid. To further confirm the formation of Ery induced imprints in the polymer, the preparation of the reference sensor (NIP) was subjected to similar CV and EIS measurements. It can be seen from Fig.3.5 that while poly(mPD-co-APBA) formation resulted in similar depression of CV current peaks and increase in EIS charge transfer resistance as in the case of poly(mPD-co-APBA-Ery), the treatment with acetic acid yielded much less changes in the measured parameters, thus validating the suggestion that the removal
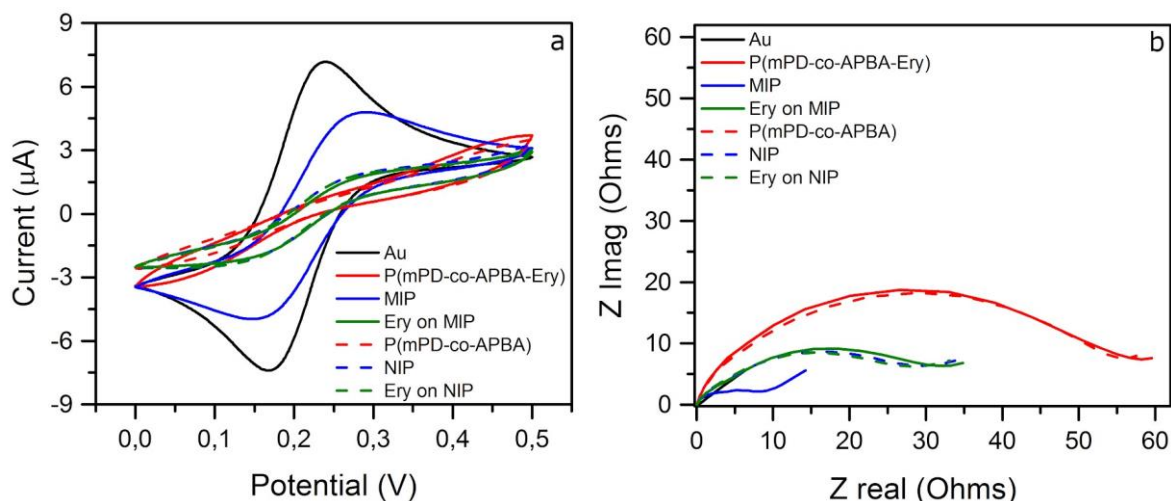
Figure 3.5. CV (a) and EIS (b) characterization of gMIP preparation on SPE. The measurements were performed in 1 M KCl solution containing 4 mM $K_3[Fe(CN)_6]/K_4[Fe(CN)_6]$.

of Ery from poly(mPD-co-APBA-Ery) resulted in the observed increase in charge transfer.

3.2 Optimization of gMIP synthesis and performance

Several parameters should be evaluated during the synthesis of a gMIP because they affect the polymer morphology, selective recognition properties, and performance of the resulting gMIP-sensor. In this study the following synthesis parameters were optimized: mPD:APBA concentration ratio, Ery:mPD:APBA concentration ratio, effect of sodium fluoride addition, and pH of polymerization solution. To assess the effect of the selected parameter on the resulting gMIP properties, the gMIP-modified SPE response signals towards a fixed concentration of Ery were recorded and compared.

3.2.1 Monomers concentration ratio

The gMIPs were synthesized using five different mPD:APBA molar ratios, namely 15:5, 10:5, 5:5, 5:10, 5:15. The gMIP-modified SPE responses upon Ery rebinding are shown in Fig. 3.6. As can be seen the highest signal belongs to the sensor modified with gMIP prepared at mPD:APBA ratio of 10:5. Consequently, this mPD:APBA molar ratio was selected as an optimal for gMIP formation.
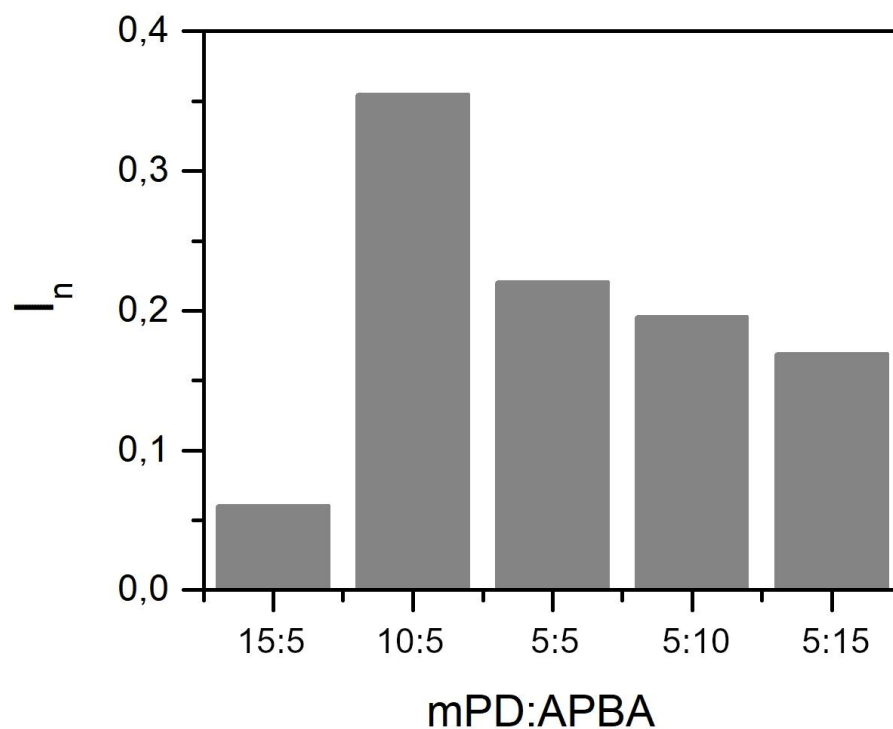
Figure 3.6. Response signals of gMIP-modified SPE upon the incubation in 40 μM Ery solution in PBS. gMIPs were prepared using different ratios of mPD:APBA (15:5, 10:5, 5:5, 5:10, and 5:15).

3.2.2 Template:monomer concentration ratio

The stoichiometric ratio of template and monomers highly influences the effectiveness of molecular imprinting. This is extremely crucial in non-covalent molecular imprinting, where the performance of gMIP is decided by pre-polymerization complexes. According to previously published studies on non-covalent imprinting, the maximal gMIP performance was achieved at the template:monomer ratio less than 1, at the same time further changes in template concentration may lead to the failures of gMIP performance optimization [63,68]. The high ratio of functional monomers to a template usually results in high non-specific affinity, whereas low ratios result in fewer complexation events because of inadequate functional groups. To study for optimum efficiency, various combinations of ratios were investigated by fixing the monomers concentration ratio mPD:APBA at 10 mM: 5 mM, and varying Ery concentration from 1 to 5 mM. As can be seen from Fig. 3.7 the highest response signal was achieved for a sensor modified with gMIP synthesized at Ery:mPD:APBA molar ratio of 2:10:5. This indicates that at this optimal concentration ratio of template to monomers, gMIP with a greater ability to selectively recognize the target at the molecular level was formed.
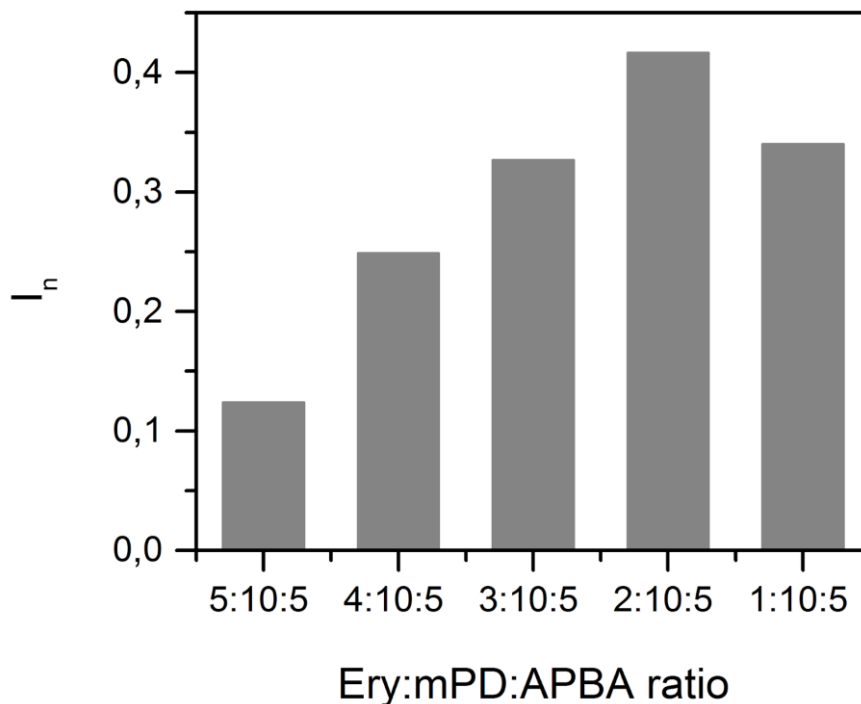
Figure 3.7. Response signals of gMIP-modified SPE upon the incubation in 40 µM Ery solution in PBS. gMIPs were prepared with various Ery:mPD:APBA ratios (5:10:5, 4:10:5, 3:10:5, 2:10:5 and 1:10:5).

3.2.3 Sodium fluoride addition

It has been previously observed that polymerization of APBA even in the form of a complex with 1,2-diols is difficult to achieve with zero or low concentration of NaF. The observation was explained as the result of intermolecular amine–boronic acid interactions that would be disrupted by the addition of fluoride. In the absence of fluoride, although an anionic tetrahedral complex may be formed between the boronic acid group and the diol, polymerization would not occur since the amine would be tied up in the complex and perhaps because of steric complications.

Thus, the electropolymerization of P(mPD-co-APBA-Ery) was carried out in the presence of low and high amounts of NaF (0, 5, 250 mM) to estimate the influence of NaF on the gMIP-modified sensor response. As shown in Fig. 3.8, the sensor response grows with increasing NaF concentration in polymerization solution. Thus, the addition of 250 mM NaF to the polymerization solution helped to generate gMIP capable of the strongest rebinding of Ery.

3.2.4 pH optimization

The effect of pH during P(mPD-co-APBA-Ery) electropolymerization on the performance of the resulting gMIP was studied. As can be seen from Fig. 3.9, the maximal current
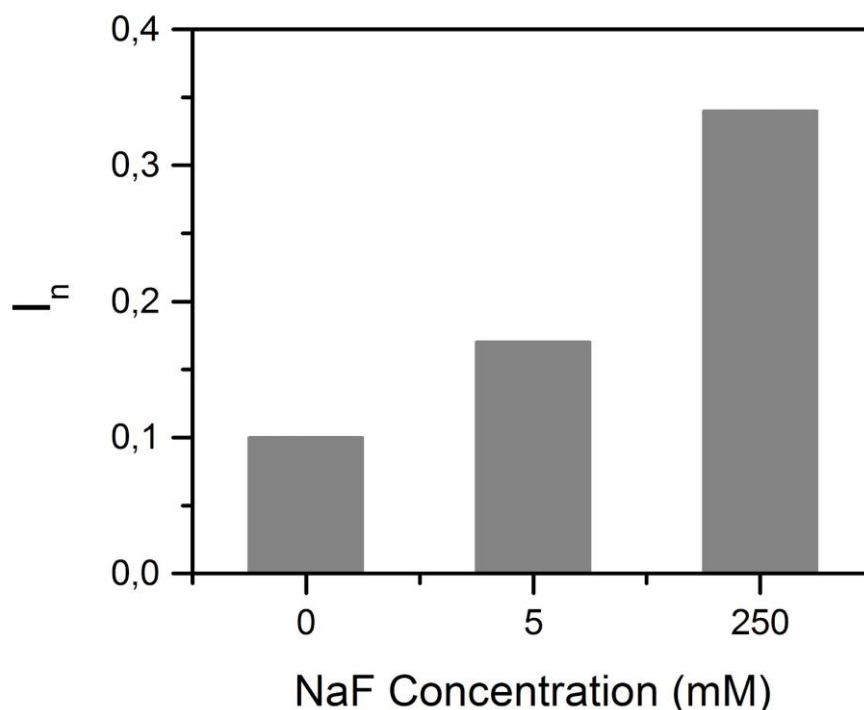
Figure 3.8. Response signals of gMIP-modified SPE upon the incubation in 40 μM Ery solution in PBS. The effect of NaF addition at concentration of 0, 5, and 250 mM to the polymerization solution for gMIP preparation.

response of gMIP-SPE sensor toward 40 μM Ery was observed in the case when gMIP was synthesized at pH 7. This indicates that the resulting gMIPs possessed higher binding affinity to Ery as compared to gMIPs prepared at lower pH. Moreover, as mentioned earlier, boronic acid has a low affinity toward diols at low pH that raises when pH is increased. Therefore, pH 7 was chosen as the optimal condition for rebinding macrolides to the gMIP-SPE sensor.

3.3 Rebinding study

To evaluate the molecular recognition properties of the prepared gMIP towards the target analytes (Ery, Cla, Azi), the rebinding study was carried out. For this purpose, the responses of the gMIP-modified sensor to the increasing analyte concentration were plotted as a function of analyte concentration to construct an adsorption isotherm. The adsorption isotherm was subsequently fitted to the Langmuir-Freundlich model (Eq. 1.6) to determine the response at maximum adsorption I_{max}, and the equilibrium dissociation constant K_D. The mathematical equation derivable from the model gives an accurate fit to the adsorption isotherms of the sensor to all analyte, thus indicating that a certain degree of heterogeneity is introduced within the polymer during imprinting [110].

Figure 3.10 shows the adsorption isotherms of both gMIP and NIP sensors to the increasing concentration of each analyte. As observed, the responses of the gMIP to each analyte is much higher than the corresponding NIP responses. This is also shown by the higher I_{max} values (1,6, 1,0 and 1,1) of the gMIP with respect to the NIP (0,3, 0,2 and 0,2), Table 3.1. To better appreciate the gMIP performance, the relative adsorption capacities computed from the IF (Eq. 1.7) were obtained. As seen in Table 3.1, the sensor demonstrates approximately 5 times higher responses for all analytes than the NIP. This clearly suggests that the binding sites created within the polymer significantly contribute to each analyte recognition.

Table 3.1 Parameters derived from fitting the Ery adsorption with Langmuir-Freundlich isotherm.

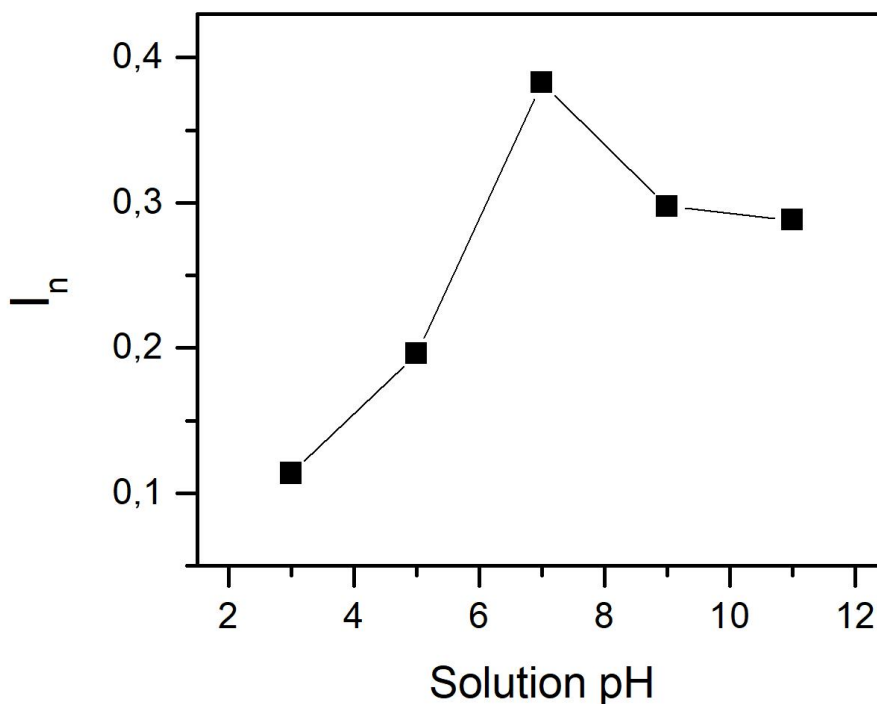| Fitting Parameters	Ery		Cla		Azi	
	gMIP	NIP	gMIP	NIP	gMIP	NIP
I_{max}	1,6 ± 0,2	0,3 ± 0	1,0 ± 0,1	0,2 ± 0,1	1,1 ± 0,1	0,2 ± 0,1
K_D (µM)	8,4	8,8	2,1	5,2	5,1	3,2
m	0,3	0,4	0,3	0,5	0,4	0,4
IF	5,3		5,0		5,5	
R^2	0,9894		0,9956		0,9908	

Figure 3.9. Response signals of gMIP-modified SPE upon the incubation in 40 µM Ery solution in PBS. gMIPs were prepared at different pH values (pH 3, pH 5, pH 7, pH 9, pH 11).
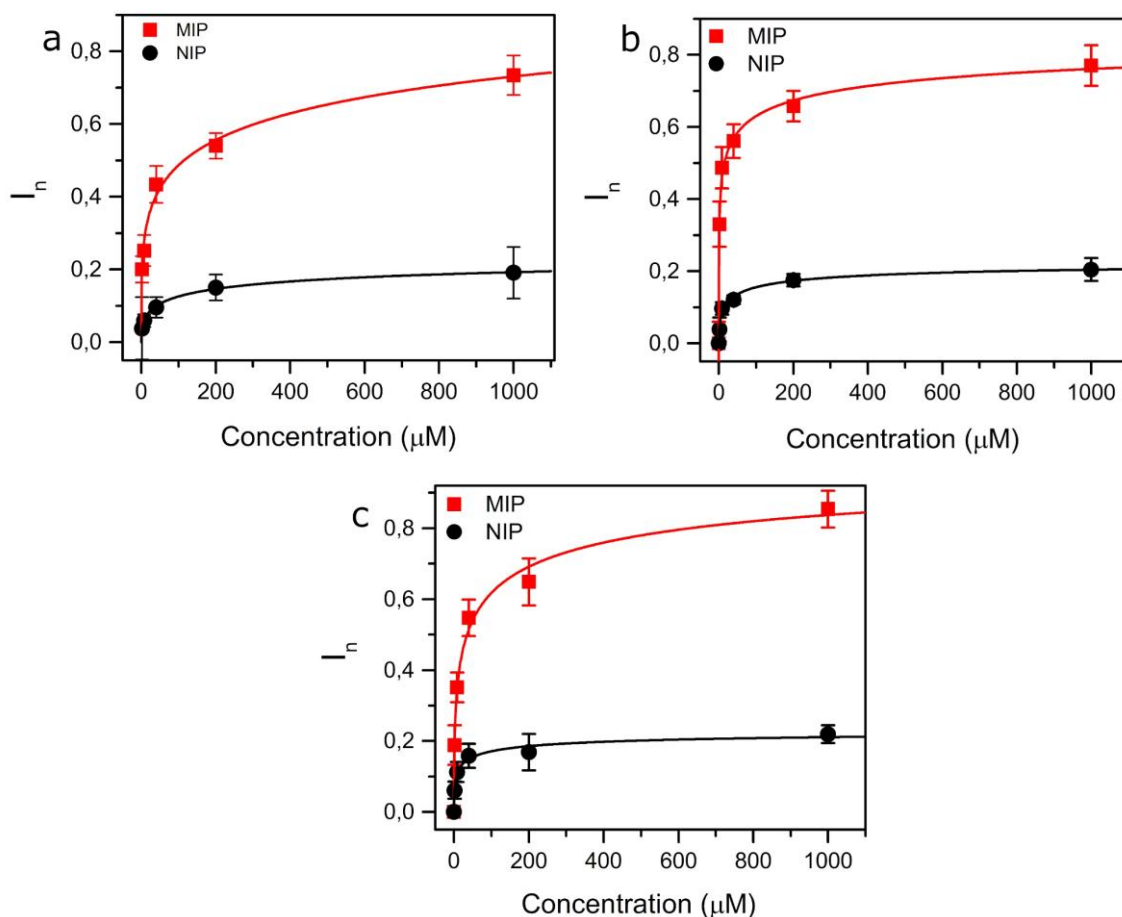
Figure 3.10. Binding isotherms of a: Ery, b: Cla, c: Azi to the gMIP and NIP-modified SPEs following with 1,6 to 1000 µM in PBS buffer, fitted by Langmuir-Freundlich isotherm.

3.4 Group-selectivity of the prepared gMIPs

The interfering molecules may affect the performance of a gMIP sensor by interacting with the gMIP binding sites when measuring environmental samples. Selectivity, or the ability to preferentially bind to the target in the presence of interfering molecules, is one of the factors deciding the quality of a MIP sensor. Selectivity study was conducted by measuring the responses of gMIP and NIP sensors upon incubation in individual solutions of 6 different antibiotics: Cipro, Amo, SMZ, Ery, Cla, and Azi. While Ery, Cla, Azi are macrolide antibiotics, the three others belong to different antibiotic groups: Cipro - to quinolone, Amo - to beta-lactam, and SMZ - to sulfonamide groups. The results showed that gMIP had a stronger response to Ery, Cla, and Azi than to Cipro, Amo, and SMZ (Fig. 3.10). The higher NIP signals of Ery, Cla, and Azi compared to others can be attributed to non-specific responses of functional monomers towards macrolides. Thus, the results indicated that prepared gMIPs had a very high recognition capacity towards macrolides and demonstrated their appreciable discrimination against interfering compounds.
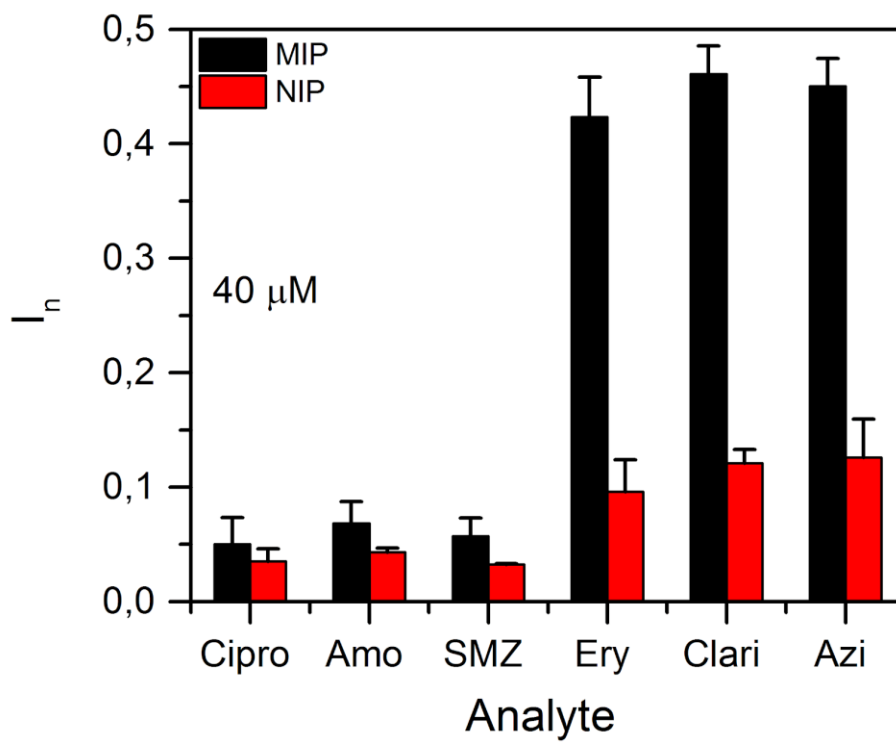
Figure 3.10. Response signals obtained from incubation of gMIP and NIP sensors in 40µM of different antibiotics (Cipro; AMO; SMZ; Ery; Clari; Azi) in PBS.

SUMMARY

In this thesis, a gMIP based recognition film was prepared on a screen-printed electrode (SPE) to achieve an electrochemical sensor for detecting macrolide group of antibiotics that are commonly presented in the EU's surface water watch list of environmental pollutants (Ery, Cla, and Azi). The following summary can be drawn from the study:

●   Two monomers including meta-phenylenediamine (mPD) and 3-aminophenyl boronic acid (APBA) were chosen as electro-polymerizable functional monomers to create macrolide imprints within poly(mPD-co-APBA). While mPD provides a non-covalent interaction (via H-bond) with the template (Ery), APBA interacts covalently through the formation of boronate ester complex by the interaction of boronic acid and diols.

●   Optimization of gMIP preparation indicates that the gMIP performance is affected by the molar ratio between template and functional monomers, concentration of NaF and the pH of solution. Thus, the optimal conditions for synthesizing a macrolide selective gMIP were found to include an Ery: mPD: APBA molar ratio of 2:10:5 mM, 250 mM NaF, and a pH of about 7.

●   The rebinding of each macrolide (Ery, Cla, Azi) on the sensor was modelled by the Langmuir-Freundlich adsorption equation which revealed approximately 5 times higher rebinding responses for each analyte than the corresponding reference sensor, NIP.

●   The prepared sensor showed remarkable selectivity for Ery, Cla, Azi against other non-macrolide compounds such as Cipro, Amo, and SMZ.

In conclusion, this thesis has demonstrated the achievement of the main goal of the research which is to develop gMIP for macrolide class of antibiotics by using two functional monomers to enhance the selective recognition of the target macrolides. To further establish the potential usability of the sensor for the intended application, future research would focus on testing the sensor in real media (e.g samples from surface, river, and underground water) as well as establishing its point of testing capability.

LIST OF REFERENCES

[1]   I. Belghadr, G. Shams Khorramabadi, H. Godini, M. Almasian, The removal of the cefixime antibiotic from aqueous solution using an advanced oxidation process (UV/H2O2), Desalination Water Treat. 55 (2015) 1068–1075. https://doi.org/10.1080/19443994.2014.928799.

[2]   Q. Chang, W. Wang, G. Regev-Yochay, M. Lipsitch, W.P. Hanage, Antibiotics in agriculture and the risk to human health: how worried should we be?, Evol. Appl. 8 (2015) 240–247. https://doi.org/10.1111/eva.12185.

[3]   A. Karkman, K. Pärnänen, D.G.J. Larsson, Fecal pollution can explain antibiotic resistance gene abundances in anthropogenically impacted environments, Nat. Commun. 10 (2019) 80. https://doi.org/10.1038/s41467-018-07992-3.

[4]   World Health Organization (WHO), Antibiotic Resistance, 2021. https://www.who.int/news-room/fact-sheets/detail/antibiotic-resistance (accessed March 30, 2021).

[5]   M. Seifrtová, L. Nováková, C. Lino, A. Pena, P. Solich, An overview of analytical methodologies for the determination of antibiotics in environmental waters, Anal. Chim. Acta. 649 (2009) 158–179. https://doi.org/10.1016/j.aca.2009.07.031.

[6]   O.S. Ahmad, T.S. Bedwell, C. Esen, A. Garcia-Cruz, S.A. Piletsky, Molecularly Imprinted Polymers in Electrochemical and Optical Sensors, Trends Biotechnol. 37 (2019) 294–309. https://doi.org/10.1016/j.tibtech.2018.08.009.

[7]   R. Crapnell, A. Hudson, C. Foster, K. Eersels, B. van Grinsven, T. Cleij, C. Banks, M. Peeters, Recent Advances in Electrosynthesized Molecularly Imprinted Polymer Sensing Platforms for Bioanalyte Detection, Sensors. 19 (2019) 1204. https://doi.org/10.3390/s19051204.

[8]   J.W. Lowdon, H. Diliën, P. Singla, M. Peeters, T.J. Cleij, B. van Grinsven, K. Eersels, MIPs for commercial application in low-cost sensors and assays – An overview of the current status quo, Sens. Actuators B Chem. 325 (2020) 128973. https://doi.org/10.1016/j.snb.2020.128973.

[9]   A. G. Ayankojo, Molecularly Imprinted Polymers Designed To Detect Antibiotic Pollutants In Water, Doctoral thesis, Tallinn University of Technology, 2018.

[10]   G. Selvolini, G. Marrazza, MIP-Based Sensors: Promising New Tools for Cancer Biomarker Determination, Sensors. 17 (2017). https://doi.org/10.3390/s17040718.

[11]   P. Rebelo, E. Costa-Rama, I. Seguro, J.G. Pacheco, H.P.A. Nouws, M.N.D.S. Cordeiro, C. Delerue-Matos, Molecularly imprinted polymer-based electrochemical sensors for environmental analysis, Biosens. Bioelectron. 172 (2021) 112719. https://doi.org/10.1016/j.bios.2020.112719.

[12] A.G. Ayankojo, J. Reut, V. Ciocan, A. Öpik, V. Syritski, Molecularly imprinted polymer-based sensor for electrochemical detection of erythromycin, Talanta. 209 (2020) 120502. https://doi.org/10.1016/j.talanta.2019.120502.

[13] S. Xizhi, S. Song, A. Sun, J. Liu, D. Li, J. Chen, Characterisation and application of molecularly imprinted polymers for group-selective recognition of antibiotics in food samples, The Analyst. 137 (2012) 3381–9. https://doi.org/10.1039/c2an35213c.

[14] E.N. Ndunda, B. Mizaikoff, Molecularly imprinted polymers for the analysis and removal of polychlorinated aromatic compounds in the environment: a review, Analyst. 141 (2016) 3141–3156. https://doi.org/10.1039/C6AN00293E.

[15] X. Chen, Z. Zhang, X. Yang, Y. Liu, J. Li, M. Peng, S. Yao, Novel molecularly imprinted polymers based on multiwalled carbon nanotubes with bifunctional monomers for solid-phase extraction of rhein from the root of kiwi fruit, J. Sep. Sci. 35 (2012) 2414–2421. https://doi.org/10.1002/jssc.201101000.

[16] H. Surikumaran, S. Mohamad, N. Muhamad Sarih, M. Ramachandran, β-Cyclodextrin Based Molecularly Imprinted Solid Phase Extraction for Class Selective Extraction of Priority Phenols in Water Samples, Sep. Sci. Technol. 50 (2015). https://doi.org/10.1080/01496395.2015.1043016.

[17] K. Zhao, T. He, S. Wu, S. Wang, B. Dai, Q. Yang, Y. Lei, Research on video classification method of key pollution sources based on deep learning, J. Vis. Commun. Image Represent. 59 (2019) 283–291. https://doi.org/10.1016/j.jvcir.2019.01.015.

[18] L. Carroll, Chapter 1 - Pollution and Environmental Ethics, in: J.J. Peirce, R.F. Weiner, P.A. Vesilind (Eds.), Environ. Pollut. Control Fourth Ed., Butterworth-Heinemann, Woburn, 1998: pp. 1–14. https://doi.org/10.1016/B978-075069899-3/50001-8.

[19] A. Dwivedi, RESEARCHES IN WATER POLLUTION: A REVIEW, 2017. https://doi.org/10.13140/RG.2.2.12094.08002.

[20] M. Kumar, P. Borah, P. Devi, Chapter 3 - Priority and emerging pollutants in water, in: P. Devi, P. Singh, S.K. Kansal (Eds.), Inorg. Pollut. Water, Elsevier, 2020: pp. 33–49. https://doi.org/10.1016/B978-0-12-818965-8.00003-2.

[21] A. Inyinbor, B. Adebesin, A. Oluyori, T. Adelani-Akande, A.O. Dada, O. A., Water Pollution: Effects, Prevention, and Climatic Impact, in: 2018. https://doi.org/10.5772/intechopen.72018.

[22] A. Ahamad, S. Madhav, A. Singh, A. Kumar, P. Singh, Types of Water Pollutants: Conventional and Emerging, in: 2019: pp. 21–41. https://doi.org/10.1007/978-981-15-0671-0_3.

[23] A. Tarfiei, H. Eslami, A.A. Ebrahimi, Pharmaceutical Pollution in the Environment and Health Hazards (JEHSD), J Env. Health Sustain Dev. 3 (2018) 492–495.

[24] N. Taoufik, W. Boumya, F.Z. Janani, A. Elhalil, F.Z. Mahjoubi, N. Barka, Removal of emerging pharmaceutical pollutants: A systematic mapping study review, J. Environ. Chem. Eng. 8 (2020) 104251. https://doi.org/10.1016/j.jece.2020.104251.

[25] V. Chander, B. Sharma, V. Negi, R.S. Aswal, P. Singh, R. Singh, R. Dobhal, Pharmaceutical Compounds in Drinking Water, J. Xenobiotics. 6 (2016) 5774–5774. https://doi.org/10.4081/xeno.2016.5774.

[26] C.L. Ventola, The antibiotic resistance crisis: part 1: causes and threats, P T Peer-Rev. J. Formul. Manag. 40 (2015) 277–283.

[27] B. Ligon, Penicillin: Its Discovery and Early Development, Semin. Pediatr. Infect. Dis. 15 (2004) 52–7. https://doi.org/10.1053/j.spid.2004.02.001.

[28] M.Lindsay. Grayson, Kucers' the use of antibiotics : a clinical review of antibacterial, antifungal, antiparasitic and antiviral drugs., 6th ed., Hodder Arnold, London, 2010. https://ljmu-primo.hosted.exlibrisgroup.com/openurl/44JMU/44JMU_services_page?u.ignore_date_coverage=true&rft.mms_id=9911235758303826.

[29] S.A. Kraemer, A. Ramachandran, G.G. Perron, Antibiotic Pollution in the Environment: From Microbial Ecology to Public Policy, Microorganisms. 7 (2019) 180. https://doi.org/10.3390/microorganisms7060180.

[30] O.O. Diallo, S.A. Baron, C. Abat, P. Colson, H. Chaudet, J.-M. Rolain, Antibiotic resistance surveillance systems: A review, J. Glob. Antimicrob. Resist. 23 (2020) 430–438. https://doi.org/10.1016/j.jgar.2020.10.009.

[31] L. Brown, C. Langelier, M.J.A. Reid, R.L. Rutishauser, L. Strnad, Antimicrobial Resistance: A Call to Action!, Clin. Infect. Dis. Off. Publ. Infect. Dis. Soc. Am. 64 (2017) 106–107. https://doi.org/10.1093/cid/ciw678.

[32] A. Faleye, A. Adegoke, K. Ramluckan, F. Bux, T. Stenström, Antibiotic Residue in the Aquatic Environment: Status in Africa, Open Chem. 16 (2018) 890–903. https://doi.org/10.1515/chem-2018-0099.

[33] Y. Ben, M. Hu, X. Zhang, S. Wu, M.H. Wong, M. Wang, C.B. Andrews, C. Zheng, Efficient detection and assessment of human exposure to trace antibiotic residues in drinking water, Water Res. 175 (2020) 115699. https://doi.org/10.1016/j.watres.2020.115699.

[34] S. Rodriguez-Mozaz, I. Vaz-Moreira, S. Varela Della Giustina, M. Llorca, D. Barceló, S. Schubert, T.U. Berendonk, I. Michael-Kordatou, D. Fatta-Kassinos, J.L. Martinez, C. Elpers, I. Henriques, T. Jaeger, T. Schwartz, E. Paulshus, K. O'Sullivan, K.M.M. Pärnänen, M. Virta, T.T. Do, F. Walsh, C.M. Manaia, Antibiotic

residues in final effluents of European wastewater treatment plants and their impact on the aquatic environment, Environ. Int. 140 (2020) 105733. https://doi.org/10.1016/j.envint.2020.105733.

[35] E. Felis, J. Kalka, A. Sochacki, K. Kowalska, S. Bajkacz, M. Harnisz, E. Korzeniewska, Antimicrobial pharmaceuticals in the aquatic environment - occurrence and environmental implications, Eur. J. Pharmacol. 866 (2020) 172813. https://doi.org/10.1016/j.ejphar.2019.172813.

[36] Joint Research Centre - European Commission's science and knowledge service, Updated surface water Watch List adopted by the Commission, (2018). https://ec.europa.eu/jrc/en/science-update/updated-surface-water-watch-list-adopted-commission.

[37] T. Golkar, M. Zieliński, A.M. Berghuis, Look and Outlook on Enzyme-Mediated Macrolide Resistance, Front. Microbiol. 9 (2018) 1942. https://doi.org/10.3389/fmicb.2018.01942.

[38] M. Gaynor, A. Mankin, Macrolide Antibiotics: Binding Site, Mechanism of Action, Resistance, Curr. Top. Med. Chem. 3 (2003) 949–61. https://doi.org/10.2174/1568026033452159.

[39] H. Kirst, Introduction to the macrolide antibiotics, (2002). https://doi.org/10.1007/978-3-0348-8105-0_1.

[40] George Dinos, The macrolide antibiotic renaissance, Br. J. Pharmacol. 174 (2017) 2967–2983. https://doi.org/10.1111/bph.13936.

[41] X. Song, T. Zhou, J. Li, M. Zhang, J. Xie, L. He, Determination of Ten Macrolide Drugs in Environmental Water Using Molecularly Imprinted Solid-Phase Extraction Coupled with Liquid Chromatography-Tandem Mass Spectrometry, Mol. Basel Switz. 23 (2018) 1172. https://doi.org/10.3390/molecules23051172.

[42] K. Farzam, T.A. Nessel, J. Quick, Erythromycin, StatPearls Publishing, Treasure Island (FL), 2020. http://europepmc.org/abstract/MED/30335282.

[43] C.-M. Wang, F.-L. Zhao, L. Zhang, X.-Y. Chai, Q.-G. Meng, Synthesis and Antibacterial Evaluation of a Series of 11,12-Cyclic Carbonate Azithromycin-3-O-descladinosyl-3-O-carbamoyl Glycosyl Derivatives, Molecules. 22 (2017) 2146. https://doi.org/10.3390/molecules22122146.

[44] E.L. Cyphert, J.D. Wallat, J.K. Pokorski, H.A. von Recum, Erythromycin Modification That Improves Its Acidic Stability while Optimizing It for Local Drug Delivery, Antibiot. Basel Switz. 6 (2017) 11. https://doi.org/10.3390/antibiotics6020011.

[45] R. Karaman, Commonly Used Drugs - Uses, Side Effects, Bioavailability & Approaches to Improve it, 2015. https://doi.org/10.13140/RG.2.1.1444.4640.

[46] R. Kumaresan, B. Regmi, Effects Of Clarithromycin On Cardiovascular System-A Review, Int. J. Pharm. Clin. Res. 9 (2019) 12–14.

[47] S. Douthwaite, S. Champney, Structures of ketolides and macrolides determine their mode of interaction with the ribosomal target site, J. Antimicrob. Chemother. 48 Suppl T1 (2001) 1–8. https://doi.org/10.1093/jac/48.suppl_2.1.

[48] J. McCarty, Azithromycin (Zithromax), Infect. Dis. Obstet. Gynecol. 4 (1996) 215–20. https://doi.org/10.1155/S1064744996000415.

[49] A. Martín-Esteban, B. Sellergren, 2.17 - Molecularly Imprinted Polymers, in: J. Pawliszyn (Ed.), Compr. Sampl. Sample Prep., Academic Press, Oxford, 2012: pp. 331–344. https://doi.org/10.1016/B978-0-12-381373-2.00046-6.

[50] M. Fizir, A. Richa, H. He, S. Touil, M. Brada, L. Fizir, A mini review on molecularly imprinted polymer based halloysite nanotubes composites: innovative materials for analytical and environmental applications, Rev. Environ. Sci. Biotechnol. 19 (2020) 241–258. https://doi.org/10.1007/s11157-020-09537-x.

[51] G. Vasapollo, R.D. Sole, L. Mergola, M.R. Lazzoi, A. Scardino, S. Scorrano, G. Mele, Molecularly imprinted polymers: present and future prospective, Int. J. Mol. Sci. 12 (2011) 5908–5945. https://doi.org/10.3390/ijms12095908.

[52] B. Fresco-Cala, A.D. Batista, S. Cárdenas, Molecularly Imprinted Polymer Micro- and Nano-Particles: A Review, Molecules. 25 (2020). https://doi.org/10.3390/molecules25204740.

[53] A. Azizi, C.S. Bottaro, A critical review of molecularly imprinted polymers for the analysis of organic pollutants in environmental water samples, J. Chromatogr. A. 1614 (2020) 460603. https://doi.org/10.1016/j.chroma.2019.460603.

[54] J. Pan, W. Chen, Y. Ma, G. Pan, Molecularly imprinted polymers as receptor mimics for selective cell recognition, Chem Soc Rev. 47 (2018) 5574–5587. https://doi.org/10.1039/C7CS00854F.

[55] M.R. Gama, C.B.G. Bottoli, Molecularly imprinted polymers for bioanalytical sample preparation, Extr. Sample Prep. Tech. Bioanal. 1043 (2017) 107–121. https://doi.org/10.1016/j.jchromb.2016.09.045.

[56] Y. Yang, X. Liu, B. Xu, Recent advances in molecular imprinting technology for the deep desulfurization of fuel oils, New Carbon Mater. 29 (2014) 1–14. https://doi.org/10.1016/S1872-5805(14)60121-9.

[57] F. Yemis, P. Alkan, B. Yenigül, M. Yenigul, Molecularly Imprinted Polymers and Their Synthesis by Different Methods, Polym. Polym. Compos. 21 (2013) 145–150. https://doi.org/10.1177/096739111302100304.

[58] E. Yilmaz, B. Garipcan, H. Patra, L. Uzun, Molecular Imprinting Applications in Forensic Science, Sensors. 17 (2017) 691. https://doi.org/10.3390/s17040691.

[59] M. Gao, Y. Gao, G. Chen, X. Huang, X. Xu, J. Lv, J. Wang, D. Xu, G. Liu, Recent Advances and Future Trends in the Detection of Contaminants by Molecularly Imprinted Polymers in Food Samples, Front. Chem. 8 (2020) 616326–616326. https://doi.org/10.3389/fchem.2020.616326.

[60] Y. Saylan, S. Akgönüllü, H. Yavuz, S. Ünal, A. Denizli, Molecularly Imprinted Polymer Based Sensors for Medical Applications, Sensors. 19 (2019) 1279. https://doi.org/10.3390/s19061279.

[61] G. Ayankojo, J. Reut, A. Öpik, A. Furchner, V. Syritski, Hybrid Molecularly Imprinted Polymer for Amoxicillin Detection, Biosens. Bioelectron. 118 (2018) 102. https://doi.org/10.1016/j.bios.2018.07.042.

[62] C. Feiyun, Z. Zhou, H.S. Zhou, Molecularly Imprinted Polymers and Surface Imprinted Polymers Based Electrochemical Biosensor for Infectious Diseases, Sensors. 20 (2020) 996. https://doi.org/10.3390/s20040996.

[63] R. Keçili, C.M. Hussain, Recent Progress of Imprinted Nanomaterials in Analytical Chemistry, Int. J. Anal. Chem. 2018 (2018) 8503853. https://doi.org/10.1155/2018/8503853.

[64] E.N. Ndunda, Molecularly imprinted polymers—A closer look at the control polymer used in determining the imprinting effect: A mini review, J. Mol. Recognit. 33 (2020) e2855. https://doi.org/10.1002/jmr.2855.

[65] L. Liu, D. Mandler, Electrochemical Deposition of Sol-Gel Films, in: L. Klein, M. Aparicio, A. Jitianu (Eds.), Handb. Sol-Gel Sci. Technol. Process. Charact. Appl., Springer International Publishing, Cham, 2018: pp. 531–568. https://doi.org/10.1007/978-3-319-32101-1_113.

[66] L. Chen, X. Wang, W. Lu, X. Wu, J. Li, Molecular imprinting: perspectives and applications, Chem. Soc. Rev. 45 (2016) 2137–2211. https://doi.org/10.1039/C6CS00061D.

[67] G. Fomo, T. Waryo, U. Feleni, P. Baker, E. Iwuoha, Electrochemical Polymerization, in: M.A. Jafar Mazumder, H. Sheardown, A. Al-Ahmed (Eds.), Funct. Polym., Springer International Publishing, Cham, 2019: pp. 105–131. https://doi.org/10.1007/978-3-319-95987-0_3.

[68] Q. Zhao, H. Zhao, W. Huang, X. Yang, L. Yao, J. Liu, J. Li, J. Wang, Dual functional monomer surface molecularly imprinted microspheres for polysaccharide recognition in aqueous solution, Anal Methods. 11 (2019) 2800–2808. https://doi.org/10.1039/C9AY00132H.

[69] E. Ndunda, B. Mizaikoff, Molecularly imprinted polymers for the detection of polychlorinated aromatic constituents in the environment: A review, The Analyst. 141 (2016). https://doi.org/10.1039/C6AN00293E.

[70] A. Kidakova, J. Reut, R. Boroznjak, A. Öpik, V. Syritski, Advanced sensing materials based on molecularly imprinted polymers towards developing point-of-care diagnostics devices, Proc. Est. Acad. Sci. 68 (2019) 158. https://doi.org/10.3176/proc.2019.2.07.

[71] V. Pichon, F. Chapuis-Hugon, Role of molecularly imprinted polymers for selective determination of environmental pollutants—A review, Anal. Chim. Acta. 622 (2008) 48–61. https://doi.org/10.1016/j.aca.2008.05.057.

[72] P.S. Sharma, A. Garcia-Cruz, M. Cieplak, K.R. Noworyta, W. Kutner, 'Gate effect' in molecularly imprinted polymers: the current state of understanding, Electrochem. Mater. Eng. 16 (2019) 50–56. https://doi.org/10.1016/j.coelec.2019.04.020.

[73] A. Yarman, F.W. Scheller, How Reliable Is the Electrochemical Readout of MIP Sensors?, Sensors. 20 (2020) 2677. https://doi.org/10.3390/s20092677.

[74] F.W. Scheller, X. Zhang, A. Yarman, U. Wollenberger, R.E. Gyurcsányi, Molecularly imprinted polymer-based electrochemical sensors for biopolymers, Bioelectrochemistry. 14 (2019) 53–59. https://doi.org/10.1016/j.coelec.2018.12.005.

[75] A. Florea, C. Cristea, F. Vocanson, R. Săndulescu, N. Jaffrezic-Renault, Electrochemical sensor for the detection of estradiol based on electropolymerized molecularly imprinted polythioaniline film with signal amplification using gold nanoparticles, Electrochem. Commun. 59 (2015) 36–39. https://doi.org/10.1016/j.elecom.2015.06.021.

[76] B. Feier, A. Blidar, A. Pusta, P. Carciuc, C. Cristea, Electrochemical Sensor Based on Molecularly Imprinted Polymer for the Detection of Cefalexin, Biosensors. 9 (2019). https://doi.org/10.3390/bios9010031.

[77] S. Di Masi, A. Garcia-Cruz, F. Canfarotta, T. Cowen, P. Marote, C. Malitesta, S. Piletsky, Synthesis and Application of Ion-Imprinted Nanoparticles in Electrochemical Sensors for Copper (II) Determination, ChemNanoMat. 5 (2019). https://doi.org/10.1002/cnma.201900056.

[78] X. Cetó, C.P. Saint, C.W.K. Chow, N.H. Voelcker, B. Prieto-Simón, Electrochemical detection of N-nitrosodimethylamine using a molecular imprinted polymer, Sens. Actuators B Chem. 237 (2016) 613–620. https://doi.org/10.1016/j.snb.2016.06.136.

[79] Z. Taleat, A. Khoshroo, M. Mazloum-Ardakani, Screen-printed electrodes for biosensing: a review (2008–2013), Microchim. Acta. 181 (2014) 865–891. https://doi.org/10.1007/s00604-014-1181-1.

[80] K.K. Mistry, K. Layek, A. Mahapatra, C. RoyChaudhuri, H. Saha, A review on amperometric-type immunosensors based on screen-printed electrodes, Analyst. 139 (2014) 2289–2311. https://doi.org/10.1039/C3AN02050A.

[81] J.K. Jadav, V.V. Umrania, K.J. Rathod, B.A. Golakiya, Development of silver/carbon screen-printed electrode for rapid determination of vitamin C from fruit juices, LWT. 88 (2018) 152–158. https://doi.org/10.1016/j.lwt.2017.10.005.

[82] N. Elgrishi, K. Rountree, B. Mccarthy, E. Rountree, T. Eisenhart, J. Dempsey, A Practical Beginner's Guide to Cyclic Voltammetry, J. Chem. Educ. 95 (2017). https://doi.org/10.1021/acs.jchemed.7b00361.

[83] P. Joshi, D.S. Sutrave, A Brief Study of Cyclic Voltammetry and Electrochemical Analysis, Int. J. ChemTech Res. 11 (2018) 77–88. https://doi.org/10.20902/IJCTR.2018.110911.

[84] A. Molina, E. Laborda, F. Martínez-Ortiz, D.F. Bradley, D.J. Schiffrin, R.G. Compton, Comparison between double pulse and multipulse differential techniques, J. Electroanal. Chem. 659 (2011) 12–24. https://doi.org/10.1016/j.jelechem.2011.04.012.

[85] K. Scott, 2 - Electrochemical principles and characterization of bioelectrochemical systems, in: K. Scott, E.H. Yu (Eds.), Microb. Electrochem. Fuel Cells, Woodhead Publishing, Boston, 2016: pp. 29–66. https://doi.org/10.1016/B978-1-78242-375-1.00002-2.

[86] F. Ruiz Simões, M.G. Xavier, Electrochemical Sensors, in: Nanosci. Its Appl., 2017: pp. 155–178. https://doi.org/10.1016/B978-0-323-49780-0.00006-5.

[87] E. Randviir, C. Banks, Electrochemical impedance spectroscopy: An overview of bioanalytical applications, Anal. Methods. 5 (2013) 1098–1115. https://doi.org/10.1039/c3ay26476a.

[88] J.M. McIntyre, H.Q. Pham, Electrochemical impedance spectroscopy; a tool for organic coatings optimizations, Proc. 20th Int. Conf. Org. Coat. Sci. Technol. 27 (1996) 201–207. https://doi.org/10.1016/0300-9440(95)00532-3.

[89] M. Ates, Review study of electrochemical impedance spectroscopy and equivalent electrical circuits of conducting polymers on carbon surfaces, Prog. Org. Coat. 71 (2011) 1–10. https://doi.org/10.1016/j.porgcoat.2010.12.011.

[90] F. Ciucci, Modeling electrochemical impedance spectroscopy, Fundam. Theor. Electrochem. 13 (2019) 132–139. https://doi.org/10.1016/j.coelec.2018.12.003.

[91] M. Orazem, B. Tribollet, Tribollet, B.: Electrochemical Impedance Spectroscopy. Wiley-Interscience, New York, 2008. https://doi.org/10.1002/9780470381588.

[92] S. El-Akaad, M. Mohamed, N. Abdelwahab, E. Abdelaleem, S. Saeger, N. Beloglazova, Capacitive sensor based on molecularly imprinted polymers for

detection of the insecticide imidacloprid in water, Sci. Rep. 10 (2020) 14479. https://doi.org/10.1038/s41598-020-71325-y.

[93] R. Umpleby, S. Baxter, Y. Chen, R. Shah, K. Shimizu, Characterization of Molecularly Imprinted Polymers with the Langmuir−Freundlich Isotherm, Anal. Chem. 73 (2001) 4584–91. https://doi.org/10.1021/ac0105686.

[94] A.G. Ayankojo, A. Tretjakov, J. Reut, R. Boroznjak, A. Öpik, J. Rappich, A. Furchner, K. Hinrichs, V. Syritski, Molecularly Imprinted Polymer Integrated with a Surface Acoustic Wave Technique for Detection of Sulfamethizole, Anal. Chem. 88 (2016) 1476–1484. https://doi.org/10.1021/acs.analchem.5b04735.

[95] G.P. Jeppu, T.P. Clement, A modified Langmuir-Freundlich isotherm model for simulating pH-dependent adsorption effects, Sorpt. Transp. Process. Affect. Fate Environ. Pollut. Subsurf. 129–130 (2012) 46–53. https://doi.org/10.1016/j.jconhyd.2011.12.001.

[96] M.G. Plaza, I. Durán, N. Querejeta, F. Rubiera, C. Pevida, Experimental and Simulation Study of Adsorption in Postcombustion Conditions Using a Microporous Biochar. 1. CO_2 and N_2 Adsorption, Ind. Eng. Chem. Res. 55 (2016) 3097–3112. https://doi.org/10.1021/acs.iecr.5b04856.

[97] A.C.M. Pássaro, T.M. Mozetic, J.E. Schmitz, I.J. da Silva, T.D. Martins, I.T.L. Bresolin, Human Immunoglobulin G Adsorption in Epoxy Chitosan/Alginate Adsorbents: Evaluation of Isotherms by Artificial Neural Networks, Chem. Prod. Process Model. 14 (2019). https://doi.org/10.1515/cppm-2019-0077.

[98] A.Y.W. Lee, S.F. Lim, S.N.D. Chua, K. Sanaullah, R. Baini, M.O. Abdullah, Adsorption Equilibrium for Heavy Metal Divalent Ions (Cu^{2+}, Zn^{2+}, and Cd^{2+}) into Zirconium-Based Ferromagnetic Sorbent, Adv. Mater. Sci. Eng. 2017 (2017) 1210673. https://doi.org/10.1155/2017/1210673.

[99] F. Wang, Z. Feixue, X. Yu, Z. Feng, N. Du, Y. Zhong, X. Huang, Electrochemical synthesis of poly (3-aminophenylboronic acid) in ethylene glycol without exogenous protons, Phys Chem Chem Phys. 18 (2016). https://doi.org/10.1039/C6CP00800C.

[100] X. Zhong, H. Bai, J.-J. Xu, H. Chen, Y. Zhu, A Reusable Interface Constructed by 3-Aminophenylboronic Acid-Functionalized Multiwalled Carbon Nanotubes for Cell Capture, Release, and Cytosensing, Adv. Funct. Mater. 20 (2010) 992–999. https://doi.org/10.1002/adfm.200901915.

[101] B. Deore, M. Freund, Saccharide imprinting of poly(aniline boronic acid) in the presence of fluoride, The Analyst. 128 (2003) 803–6. https://doi.org/10.1039/B300629H.

[102] J.N. Cambre, B.S. Sumerlin, Biomedical applications of boronic acid polymers, Polymer. 52 (2011) 4631–4643. https://doi.org/10.1016/j.polymer.2011.07.057.

[103] R. Wannapob, P. Kanatharana, W. Limbut, A. Numnuam, P. Asawatreratanakul, C. Thammakhet, P. Thavarungkul, Affinity sensor using 3-aminophenylboronic acid for bacteria detection, Biosens. Bioelectron. 26 (2010) 357–364. https://doi.org/10.1016/j.bios.2010.08.005.

[104] M. Golabi, F. Kuralay, E.W.H. Jager, V. Beni, A.P.F. Turner, Electrochemical bacterial detection using poly(3-aminophenylboronic acid)-based imprinted polymer, Spec. Issue Sel. Pap. 26th Anniv. World Congr. Biosens. Part II. 93 (2017) 87–93. https://doi.org/10.1016/j.bios.2016.09.088.

[105] W. Marinaro, R. Prankerd, K. Kinnari, V. Stella, Interaction of Model Aryl- and Alkyl-Boronic Acids and 1,2-Diols in Aqueous Solution, J. Pharm. Sci. 104 (2015). https://doi.org/10.1002/jps.24346.

[106] E.A. Andreev, M.A. Komkova, V.N. Nikitina, A.A. Karyakin, Reagentless Impedimetric Sensors Based on Aminophenylboronic Acids, J. Anal. Chem. 74 (2019) 153–171. https://doi.org/10.1134/S1061934819010040.

[107] F. Dayrit, A. Dios, 1H and 13C NMR for the Profiling of Natural Product Extracts: Theory and Applications, in: 2017. https://doi.org/10.5772/intechopen.71040.

[108] E. Hatzakis, Nuclear Magnetic Resonance (NMR) Spectroscopy in Food Science: A Comprehensive Review, Compr. Rev. Food Sci. Food Saf. 18 (2018) 189–220. https://doi.org/10.1111/1541-4337.12408.

[109] Y. Chen, L. Yang, S. Xu, S. Han, S. Chu, Z. Wang, C. Jiang, Ultralight aerogel based on molecular-modified poly(m -phenylenediamine) crosslinking with polyvinyl alcohol/graphene oxide for flow adsorption, RSC Adv. 9 (2019) 22950–22956. https://doi.org/10.1039/C9RA04207E.

[110] A.G. Ayankojo, J. Reut, R. Boroznjak, A. Öpik, V. Syritski, Molecularly imprinted poly(meta-phenylenediamine) based QCM sensor for detecting Amoxicillin, Sens. Actuators B Chem. 258 (2018) 766–774. https://doi.org/10.1016/j.snb.2017.11.194.